Table 1 Alleles of *ULBP2.1* and *ULBP2.2* in rhesus and cynomolgus macaques

Gene	Species	Allele name	Accession no	ID of reference animal	Clone name
ULBP2.1	*Macaca mulatta*	*Mamu-ULBP2.1*1*	NC007861[a]	Not found in the subjects of this study	
		*Mamu-ULBP2.1*2*	AB826205	R491	UL2.1NR491F-9
		*Mamu-ULBP2.1*3*	AB826206	R312, R314, R496	UL2.1NR314F-2
		*Mamu-ULBP2.1*4*	AB826207	R277, R316, R350, R396, R429, R434, R437, R455, R465, R473, R492, R495	UL2-1R227-13 F
		*Mamu-ULBP2.1*5*	AB826208	R325, R333, R337, R384, R434, R491	UL2-1R434-2 F
		*Mamu-ULBP2.1*6*	AB826209	R350	UL2.1NR350F-13
		*Mamu-ULBP2.1*7*	AB826210	R227, R234, R283, R314, R320, R321, R328, R337, R346, R384,R396, R446, R455, R465, R490, R496	UL2-1R227-7 F
		*Mamu-ULBP2.1*8*	AB826211	R495	UL2.1NR495F-8
		*Mamu-ULBP2.1*9*	AB826212	R321, R333, R360	UL2.1NR321F-8
		*Mamu-ULBP2.1*10*	AB826213	R316, R342, R408	UL2-1R408-12 F
		*Mamu-ULBP2.1*11*	AB826214	R346	UL2.1NR346F-20
		*Mamu-ULBP2.1*12*	AB826215	R342	UL2.1NR342F-14
		*Mamu-ULBP2.1*13*	AB826216	R325, R346, R360, R361, R379, R408, R429, R430, R437, R439, R446, R473, R490	UL2.1NR439F-11
		*Mamu-ULBP2.1*14*	AB826217	R453	UL2-1R453-1 F
		*Mamu-ULBP2.1*15*	AB826204	R234, R312, R361	UL2.1NR234F-7
	Macaca fascicularis	*Mafa-ULBP2.1*1*	NC007861[a]	M04, C09	2.1-2UL2-1 M04-5 F
		*Mafa-ULBP2.1*2*	AB826219	M05, C10, C11	UL2.1NFM05-12
		*Mafa-ULBP2.1*3*	AB826220	M03, C07	UL2.1NFM03-8
		*Mafa-ULBP2.1*4*	AB826221	P01, P02, P03, M01, C01, C03, C04, C05, C07, C08	2.1-1UL2-1 M01-10 F
		*Mafa-ULBP2.1*5*	AB826222	P02, C06	UL2-1P02-2 F
		*Mafa-ULBP2.1*6*	AB826223	M02, C05	2.1-6UL2-1 M02-17 F
		*Mafa-ULBP2.1*7*	AB826224	M03, M04, C06, C08, C09	UL2-1 M03-1 F
		*Mafa-ULBP2.1*8*	AB826225	P04, P05, M01, M05, M06, C02, C12, C13	2.1-3UL2-1 M01-12 F
		*Mafa-ULBP2.1*9*	AB826226	P04, M06, C10, C11, C12, C13	2.1-4UL2-1 M06-10 F
		*Mafa-ULBP2.1*10*	AB826228	M02, C04	UL2-1 M02-20 F
		*Mafa-ULBP2.1*11*	AB826218	P01, C02	UL2NP01-F-2
ULBP2.2	*Macaca mulatta*	*Mamu-ULBP2.2*1*	NC007861[b]	R283, R316, R320, R321, R325, R328, R333, R337, R342, R346, R360, R379, R384, R396, R408, R429, R430, R437, R439, R446, R453, R473, R490, R495	UL2-2R396-3 F
		*Mamu-ULBP2.2*2*	AB827340	R491	UL2.2NR491F-5
		*Mamu-ULBP2.2*3*	AB827341	R314, R321	UL2-2R314-7 F
		*Mamu-ULBP2.2*4*	AB827342	R350	UL2.2NR350F-3
		*Mamu-ULBP2.2*5*	AB827343	R234, R320	UL2-2R361-8 F
		*Mamu-ULBP2.2*6*	AB827344	R325, R333, R337, R384, R491, R492	UL2-2R325-12 F
		*Mamu-ULBP2.2*7*	AB827345	R237, R312, R453	UL2-2R237-5 F
		*Mamu-ULBP2.2*8*	AB827346	R228, R314, R396, R492, R495	UL2-2R383-3 F
		*Mamu-ULBP2.2*9*	AB827347	R496	UL2-2R496-12 F
		*Mamu-ULBP2.2*10*	AB827339	R234, R312, R328, R439,R446, R490, R496	R234UL2.2NF-16
		*Mamu-ULBP2.2*11*	AB827348	R367, R430	UL2-2R367-12 F

Table 1 (continued)

Gene	Species	Allele name	Accession no	ID of reference animal	Clone name
	Macaca fascicularis	*Mafa-ULBP2.2*1*	NC007861[b]	M05, C10, C11	UL2-2FM05-2
		*Mafa-ULBP2.2*2*	AB827350	M03, M04, C06, C08	UL2-2FM03-1
		*Mafa-ULBP2.2*3*	AB827351	P03, C08	P03UL2-2-6 F
		*Mafa-ULBP2.2*4*	AB827352	P01, C03, C04, C05	UL2-2P01-1 F
		*Mafa-ULBP2.2*5*	AB827353	P01,P03, P04, M01, M04, M06, C01, C02, C09, C11, C13	UL2-2P01-7 F
		*Mafa-ULBP2.2*6*	AB827354	P04, P05, M05, M06, C12, C13	UL2-2P04-19 F
		*Mafa-ULBP2.2*7*	AB827355	M02, C05,	UL2-2FM02-2
		*Mafa-ULBP2.2*8*	AB827356	M03, C07	UL2-2FM03-11
		*Mafa-ULBP2.2*9*	AB828102	P02, M01, C01, C03, C06, C07	UL2-2FM01-1
		*Mafa-ULBP2.2*10*	AB827349	M02, C04	UL2-2FM02-11

[a] Identical to LOC694466

[b] Identical to LOC694600

Structure model analysis

Three-dimensional (3D) structure models of ULBP2 molecules were created for amino acid positions from 1 to191, by using a molecular visualization software RasTop2.2 (http://sourceforge.net/projects/rastop/), by referring the human ULPB3 molecule in complex with NKG2D (Radaev et al. 2001) from the Molecular Modeling Database (MMCB No.18231). Polymorphic sites were mapped on the 3D structure models by using the Cn3D 4.1 program (http://www.ncbi.nlm.nih.gov/Structure/CN3D/cn3d.shtml).

Results

Identification of alleles for a ULBP2 gene, *ULBP2.1*

There are two orthologous genes for *ULBP2*, LOC694466 and LOC694600, in the rhesus macaque genome. In the present study, we designated LOC694466 and LOC694600 as *ULBP2.1* and *ULBP 2.2*, respectively, and we designed primer pairs to separately amplify the *ULBP2.1* and *ULBP 2.2*. As expected, PCR products from each gene could be obtained and distinguished by their lengths, although minor length differences due to single nucleotide repeat number polymorphisms in an A stretch were found in the intron 2 sequences.

We obtained nucleotide sequences for the region from exon 2 to exon 3 of *ULBP2.1* from 37 rhesus macaques and 24 cynomolgus macaques by sequencing the cloned PCR products of 1,370–1,395 bp. The *ULBP2.1* sequences from the rhesus macaques were classified into 15 different alleles (Table 1), designated as *Mamu-ULBP2.1*1* to *-ULBP2.1*15*. The LOC4964466 sequences were given with the allele name of *Mamu-ULBP2.1*1*, although it was not found in the analyzed subjects of current study. In the cynomolgus macaques, 11 different alleles, *Mafa-ULBP2.1*01* to *-ULBP2.1*11*, were identified (Table 1). The nucleotide sequences of *Mafa-ULBP2.1*1* were identical to those of *Mamu-ULBP2.1*1* reported for rhesus macaque LOC694466.

Fig. 1 Phylogenetic tree of *ULBP2.1* and *ULBP2.2* alleles and related *ULBP2*. The tree was constructed using neighbor-joining method with bootstrap values of 5,000 replications. The values are indicated as percentages and those values less than 50 % are not shown. The sequences of human *ULBP2* (AY026825), human *ULBP5* (AL583835), human *ULBP6* (AL355497), rhesus *ULBP5* (LOC694265), chimpanzee *ULBP2* (NC006473), western gorilla *ULBP2* (NC018430), and olive baboon *ULBP2* (NC018155) were included in the analysis. The *underlined alleles* indicated with *triangles* and *stars* carried polymorphisms on the α helix structure and contact sites with NKG2D, respectively ▶


Mamu-ULBP2.1*12
Mamu-ULBP2.1*1 , Mafa-ULBP2.1*1, Mamu-ULBP2.1*11
96.1
Mamu-ULBP2.1*9
Mafa-ULBP2.1*6, Mafa-ULBP2.1*7, Mafa-ULBP2.1*8
Mamu-ULBP2.1*10
Mafa-ULBP2.1*9
Mafa-ULBP2.1*11
Mamu-ULBP2.1*7
Mamu-ULBP2.1*13
Mafa-ULBP2.1*2, Mafa-ULBP2.1*3, Mafa-ULBP2.1*11
86.7
Mamu-ULBP2.1*3
63.1
Mafa-ULBP2.1*4
63.6
Mamu-ULBP2.1*4, Mamu-ULBP2.1*5
Mamu-ULBP2.1*6
51.8
Mamu-ULBP2.1*8
63.2
Mamu-ULBP2.1*15
66.0
Mamu-ULBP2.1*14
Mamu-ULBP2.1*2
Mafa-ULBP2.2*4
Mafa-ULBP2.2*5
Mafa-ULBP2.2*2
Mafa-ULBP2.2*10
Mafa-ULBP2.2*3
87.3
Mamu-ULBP2.2*5
Mamu-ULBP2.2*6
63.4
Mamu-ULBP2.2*7
Mamu-ULBP2.2*2
Mafa-ULBP2.2*9
96.9
Mamu-ULBP2.2*8
Mamu-ULBP2.2*9
69.0
51.8
Mamu-ULBP2.2*3
Mamu-ULBP2.2*4
Mamu-ULBP2.2*1, Mamu-ULBP2.2*11, Mafa-ULBP2.2*1, Mafa-ULBP2.2*6
88.7
Mafa-ULBP2.2*7
99.5
Mamu-ULBP2.2*10
65.1
Olive baboon ULBP2
RhesusULBP5
Mafa-ULBP2.2*8
Mafa-ULBP2.1*5
Human ULBP5
65.8
Human ULBP2
79.7
Human ULBP6
98.7
98.8
Western gorilla ULBP2
65.7
Chimpanzee ULBP2

Table 2 Number of polymorphic sites and non-synonymous sites in ULBP2 genes in macaques and human

Locus	Number of alleles	Exon 2		Intron 2	Exon 3	
		Polymorphic sites	Non-synonymous sites (%)	Polymorphic sites	Polymorphic sites	Non-synonymous sites (%)
Mamu ULBP2.1	15	10	10 (100)	14	7	4 (57.1)
Mafa ULBP2.1	11	8	7 (87.5)	12	6	3 (50.0)
Mamu ULBP2.2	11	7	6 (85.7)	9	14	9 (64.3)
Mafa ULBP2.2	10	17	7 (41.2)	13	12	9 (75.0)
Human ULBP2	NC	17	14 (82.3)	0	15	11 (74.0)
Human ULBP6	NC	14	13 (92.9)	1	17	11 (64.7)

NC not counted because the polymorphisms in the public databases are indicated for each site and not for full sequence

Identification of alleles for another ULBP2 gene, *ULBP2.2*

PCR products for *ULBP2.2* could be obtained from genomic DNAs of both rhesus and cynomolgus macaques. Sequencing data from the cloned PCR products of 1,080–1,085 bp were classified into 11 different alleles, *Mamu-ULBP2.2*1* to *-ULBP2.2*11*, from the rhesus macaques and 10 alleles, *Mafa-ULBP2.2*1* to *-ULBP2.2*10*, from the cynomolgus

a

```
Mamu-ULBP2.1*1     1:PRWSQTGGDD PHSLCYDITI IPKFRPGPQW CAVQGQVDKK TFLHYDCGNK TVTSVSPLGK KLNVTKAWKA QNPVLREVVD MLTEQLLDIQ LENYTPREPL 100
Mamu-ULBP2.1*2      :********** ---------- ---------- ---------- ---------- ---------- ---------- ---------- ---------- ----------
Mamu-ULBP2.1*3      :********** ---------- ---------- ---------- ---------- ---------- ---------- ---------- ---------E ----------
Mamu-ULBP2.1*4      :********** ---------- ---------- ---------- ---------- ---------- ---------- ---------- ---------- ----------
Mamu-ULBP2.1*5      :********** ---------- ---------- ---------- ---------- ---------- ---------- ---------- ---------- ----------
Mamu-ULBP2.1*6      :********** L--------- ---------- ---------- ---------- ---------- ---------- ---------- ---------- ----------
Mamu-ULBP2.1*7      :********** ---------- --------R- ---------- ---------- ---------- ---------- --T------- ---------- ----------
Mamu-ULBP2.1*8      :********** ---------- ---------- ---------- ---------- ------T--- ---------- ---------- ---------- ----------
Mamu-ULBP2.1*9      :********** L--------- ---------- ---------- ---------- ----I-T--- ---------- ---------- ---------- ----------
Mamu-ULBP2.1*10     :********** L--------- ---------- Y--------- ---------- ------T--- ---------- ---------- ---------- ----------
Mamu-ULBP2.1*11     :********** ---------- ---------- ---------- ---------- ---------- ---------- ---------- ---------- ----------
Mamu-ULBP2.1*12     :********** ---------- ---------- ---------- ---------- ---------- ---------- ---------- ---------- ----------
Mamu-ULBP2.1*13     :********** ---------- ---------- ---------- ---------- ---P------ ---------- ---------- ---------- ----------
Mamu-ULBP2.1*14     :********** ---------- ---------- ---------- ---------- ---------- Q--------- ---------- ---------- ----------
Mamu-ULBP2.1*15     :********** ---------- ---------- ---------- ---------- ---------- Q--------- ---------- ---------- ----------
Mafa-ULBP2.1*1      :********** ---------- ---------- ---------- ---------- ---------- ---------- ---------- ---------- ----------
Mafa-ULBP2.1*2      :********** ---------- ---------- ----D----- ---------- ---------- ---------- ---------- ---------E ----------
Mafa-ULBP2.1*3      :********** ---------- ---------- ----D----- ---------- ---------- ---------- ---------- ---------E ----------
Mafa-ULBP2.1*4      :********** ---------- ---------- ---------- ---------- ---------- ---------- ---------- ---------- ----------
Mafa-ULBP2.1*5      :********** L--------- --------R- ---------- ---------- ---P------ ---------- ---------- ---------- ----------
Mafa-ULBP2.1*6      :********** L--------- ---------- ---------- ---------- ------T--- ---------- ---------- ---------- ----------
Mafa-ULBP2.1*7      :********** L--------- ---------- ---------- ---------- ------T--- ---------- ---------- ---------- ----------
Mafa-ULBP2.1*8      :********** L--------- ---------- ---------- ---------- ------T--- ---------- ---------- ---------- ----------
Mafa-ULBP2.1*9      :********** L-------I- ---------- ---------- ---------- ------T--- ---------- ---------- ---------- ----------
Mafa-ULBP2.1*10     :********** ---------- --------R- ----D----- ---------- ------T--- ---------- ---------- ---------- ----------
Mafa-ULBP2.1*11     :********** ---------- ---------- ---------- ---------- ---------- ---------- ---------- ---------E ----------
Mamu-ULBP2.2*1      :SL--RA-RA- L-----E--- -------RR- ---------- ---------- I--P------ --S------- ---------- ---------- ----------
Mamu-ULBP2.2*2      :********** L-----E--- -------RR- ---------- ---------- I--P----V- -FS------- ---------- ---------- ----------
Mamu-ULBP2.2*3      :********** L-----E--- -------RR- ---------- ---------- I--P------ -FS------- ---------- ---------- ----------
Mamu-ULBP2.2*4      :********** L-----E--- -------RR- ---------- ---------- I--------- -FS------- ---------- ---------- ----------
Mamu-ULBP2.2*5      :********** L-----E--- -------RR- ---------- ---------- I--PI----- -FS------- ---------- ---------- ----------
Mamu-ULBP2.2*6      :********** L-----E--- -------RR- ---------- ---------- I--PI---V- -FS------- ---------- ---------- ----------
Mamu-ULBP2.2*7      :********** L-----E--- -------RR- ---------- ---------- I--PI----- -FS------- ---------- ---------- ----------
Mamu-ULBP2.2*8      :********** L-----E--- -------RR- ---------- ---------- I--P------ -FS------- ---------- ---------- ----------
Mamu-ULBP2.2*9      :********** L-----E--- -------RR- ---------- ---------- ---P------ -FS------- ---------- ---------- ----------
Mamu-ULBP2.2*10     :********** L-----E--- -------RR- ---------- ------Y--- I--P------ -LS------- ---------- ---------- ----------
Mamu-ULBP2.2*11     :********** L-----E--- -------RR- ---------- ---------- I--P------ -LS------- ---------- ---------- ----------
Mafa-ULBP2.2*1      :********** L-----E--- -------RR- ---------- ---------- I--P------ -LS------- ---------- ---------- ----------
Mafa-ULBP2.2*2      :********** L-----E--- -------RR- ---------- ---------- I--P------ -FS------- ---------- ---------- ----------
Mafa-ULBP2.2*3      :********** L-----E--- -------RR- ---------- ---------- I--P------ -FS------- ---------- ---------- ----------
Mafa-ULBP2.2*4      :********** L-----E--- -------RR- ---------- ---------- I--P------ -FS------- ---------- ---------- ----------
Mafa-ULBP2.2*5      :********** L-----E--- -------RR- ---------- ---------- I--P------ -FS------- ---------- ---------- ----------
Mafa-ULBP2.2*6      :********** L-----E--- -------RR- ---------- ---------- I--P------ --S------- ---------- ---------- ----------
Mafa-ULBP2.2*7      :********** L-----E--- -------RR- ---------- ---------- I--P------ --S------- ---------- ---------- ----------
Mafa-ULBP2.2*8      :********** ---------- -------PR- ---------- ---------- ---P--T--- ---------- ---------- ---------- ----------
Mafa-ULBP2.2*9      :********** L-----E--- -------RR- ---------- ---------- I--P------ -FS------- ---------- ---------- ----------
Mafa-ULBP2.2*10     :********** L-----E--- -------RR- ---------- ---------- I--P------ -FS------- ---------- ---------- ----------
Human ULBP2         :SG--RA-RA- ------D--V -------PR- --------E- ---------- ---P------ -----T---- ---------- I-----R--- ------K---
Human ULBP6         :FG--RARR-- ------D--V -------PR- --------E- ---------- ---P------ -----M---- ---------- I--------- ------K---
```

Fig. 2 Alignment of deduced amino acid sequences of α1 and α2 domains of ULBP2-related molecules from rhesus and cynomolgus macaques and human. Amino acid sequences deduced from nucleotide sequences for *Mamu-ULBP2.1*1* and alleles of *Mamu-ULBP2.1*, *Mafa-ULBP2.1*, *Mamu-ULBP2.2,* and *Mafa-ULBP2.2*, were aligned with human *ULBP2* (AY026825), and *ULBP6* (AL355497). *Numbers* represent the amino acid positions in mature protein. Sequences for the predicted α helix structure are *underlined* and *contact sites* with NKG2D are *boxed* in the *Mamu-ULBP2.1*1* sequences. *Dashes* indicate identity to the *Mamu-ULBP2.1*1* sequences. *Asterisks* represent not sequenced regions. Amino acid sequences are shown **a** from 1 to 100 and **b** from 101 to 191

b

```
Mamu-ULBP2.1*1   101:TLQARMSCEQ KAEGHSSGSW QFGFDGQVFL LFDSENRMWT TVHPGARKMK EKWENDKDVT MSFHYISMGD CTRWLGDFLM DMDSTLEPSA G 191
Mamu-ULBP2.1*2      :---------- ---------- ---------- ---------- ---------- ---------- ---------- ---------- G--------- -
Mamu-ULBP2.1*3      :---------- ---------- ---------- ---------- ---------- ---------- ---------- ---------- ---------- -
Mamu-ULBP2.1*4      :---------- ---------- ---------- ---------- ---------- ---------- ---------- ------E--- ---------- -
Mamu-ULBP2.1*5      :---------- ---------- ---------- ---------- ---------- ---------- ---------- ------E--- ---------- -
Mamu-ULBP2.1*6      :---------- ---------- ---------- ---------- ---------- ---------- ---------- ------E--- ---------- -
Mamu-ULBP2.1*7      :---------- ---------- ---------- ---------- ---------- ---------- ---------- ---------- ---------- -
Mamu-ULBP2.1*8      :---------- ---------- ---------- ---------- ---------- ---------- ---------- ---------- ---------- -
Mamu-ULBP2.1*9      :---------- -T-------- ---------- ---------- ---------- ---------- ---------- ---------- ---------- -
Mamu-ULBP2.1*10     :---------- -T-------- ---------- ---------- ---------- ---------- ---------- ---------- ---------- -
Mamu-ULBP2.1*11     :---------- ---------- ---------- ---------- ---------- ---------- ---------- ---------- ---------- -
Mamu-ULBP2.1*12     :---------- ---------- ---------- ---------- --------I- ---------- ---------- ---------- ---------- -
Mamu-ULBP2.1*13     :---------- ---------- ---------- ---------- ---------- ---------- ---------- ---------- ---------- -
Mamu-ULBP2.1*14     :---------- ---------- ---------- ---------- ---------- ---------- ---------- ---------- G--------- -
Mamu-ULBP2.1*15     :---------- ---------- ---------- ---------- ---------- ---------- ---------- ---------- G--------- -
Mafa-ULBP2.1*1      :---------- ---------- ---------- ---------- ---------- ---------- ---------- ---------- ---------- -
Mafa-ULBP2.1*2      :---------- ---------- ---------- ---------- ---------- ---------- ---------- ---------- ---------- -
Mafa-ULBP2.1*3      :---------- ---------- ---------- ---------- ---------- ---------- ---------- ---------- ---------- -
Mafa-ULBP2.1*4      :---------- ---------- ---------- ---------- ---------- ---------- ---------- ---------- ---------- -
Mafa-ULBP2.1*5      :-----V---- ---------- ---------- ---------- ---------- ---------- ---------- ---------- ---------- -
Mafa-ULBP2.1*6      :---------- -T-------- ---------- ---------- ---------- ---------- ---------- ---------- ---------- -
Mafa-ULBP2.1*7      :---------- -T-------- ---------- ---------- ---------- ---------- ---------- ---------- ---------- -
Mafa-ULBP2.1*8      :---------- -T-------- ---------- ---------- ---------- ---------- ---------- ---------- ---------- -
Mafa-ULBP2.1*9      :---------- -T-------- ---------- ---------- ---------- ---------- ---------- ---------- ---------- -
Mafa-ULBP2.1*10     :---------- -----R---- ---------- ---------- ---------- ---------- ---------- ---------- ---------- -
Mafa-ULBP2.1*11     :---------- ---------- ---------- ---------- ---------- ---------- ---------- ---------- ---------- -
Mamu-ULBP2.2*1      :-----V---- -----R---- ---------- ---------- ---------- ---------- ---------- -----K---T GT-------- -
Mamu-ULBP2.2*2      :----QV---- ---------- ---------- ---------- M--------- ---Q------ ---------- -----K---- G--------- -
Mamu-ULBP2.2*3      :-----V---- ---------- ---------- ---------- ---------- ---------- ---R------ -----K---- G--------- -
Mamu-ULBP2.2*4      :-----V---- ---------- ---------- ---------- ---------- ---------- ---R------ -----K---- G--------- -
Mamu-ULBP2.2*5      :-----V---- ---------- --S------- ---------- ---------- ---------- ---------- -----K---T GT-------- -
Mamu-ULBP2.2*6      :-----V---- ---------- --S------- ---------- ---------- ---------- ---------- -----K---T GT-------- -
Mamu-ULBP2.2*7      :-----V---- -----R---- ---------- ---------- ---------- ---------- ---------- -----K---T GT-------- -
Mamu-ULBP2.2*8      :----QV---- ---------- ---------- ---------- ---------- ------R--- ---------- -----K---T GM-------- -
Mamu-ULBP2.2*9      :----QV---- ---------- ---------- ---------- ---------- ------R--- ---------- -----K---T GT-------- -
Mamu-ULBP2.2*10     :----QV---- ---------- ---------- ---------- M--------- ---Q------ ---------- -----K---T G--------- -
Mamu-ULBP2.2*11     :-----V---- -----R---- ---------- ---------- ---------- ---------- ---------- -----K---T GT-------- -
Mafa-ULBP2.2*1      :-----V---- -----R---- ---------- ---------- ---------- ---------- ---------- -----K---T GT-------- -
Mafa-ULBP2.2*2      :-----V---- ---------- ---------- ---------- ---------- ---------- ---------- -----K---- G--------- -
Mafa-ULBP2.2*3      :-----V---- ---------- ---------- ---------- ---------- ---------- ---------- -----K---- G--------- -
Mafa-ULBP2.2*4      :-----V---- ---------- ---------- ---------- ---------- ---------- ---------- -----K---- G--------- -
Mafa-ULBP2.2*5      :-----V---- ---------- ---------- ---------- ---------- ---------- ---------- -----K---- G--------- -
Mafa-ULBP2.2*6      :-----V---- -----R---- ---------- ---------- ---------- ---------- ---------- -----K---T GT-------- -
Mafa-ULBP2.2*7      :-----V---- -----R---- ---------- ---------- ---------- ---Q------ ---------- -P---K---T GT-------- -
Mafa-ULBP2.2*8      :-----V---- ---------- ---------- ---------- ---------- -------N-- ---------- -----K---T ---------- -
Mafa-ULBP2.2*9      :----QV---- ---------- ---------- ---------- ---------- ------R--- ---------- -----K---T G--------- -
Mafa-ULBP2.2*10     :-----V---- ---------- ---------- ---------- ---------- ---------- ---------- -----K---- G--------- -
Human ULBP2         :---------- ---------- --S----I-- -----K---- ---------- -------V-A -----F---- -IG--E---- G--------- -
Human ULBP6         :---------- ---------- --SI---T-- -----K---- ---------- ---------A ---------- -IG--E---- G--------- -
```

Fig. 2 continued.

macaques (Table 1). In this study, we found a repeat number polymorphism in the A stretch in intron 2 in both *ULBP2.1* and *ULBP2.2* from both rhesus and cynomolgus macaques. Polymorphisms in exons 2 and 3 and intron 2 including the repeat polymorphism were included in the allele designation. Nucleotide sequences of *Mamu-ULBP2.2*1* and *Mafa-ULBP2.2*1* were identical to those of LOC694600. That the identical *ULBP2* alleles were shared in part by both rhesus and cynomolgus macaques was consistent with a cross-breeding between these macaques as suggested by the studies of diversity in the MHC class I genes (Saito et al. 2012).

Divergence of *ULBP2* genes in the higher primates

Nucleotide sequence homologies among the alleles of *ULBP2.1* and *ULBP2.2* in rhesus and cynomolgus macaques were 94.3 and 98.7 %, respectively, suggesting that *ULBP2.2* is less diverged than *ULBP2.1*. To figure out the evolutional divergence and diversity of *ULBP2* genes in the higher primates, we conducted a neighbor-joining analysis by using nucleotide sequences of exons 2 and 3 from *ULBP2.1* and *ULBP2.2* in macaques along with sequences of corresponding region from *ULBP2* and/or *ULBP6* reported for human, chimpanzee, gorilla, and another Old World monkey, olive baboon. *ULBP5* sequences from human and rhesus were also included in the analysis. As shown in Fig. 1, alleles of *ULBP2.1* and those of *ULBP2.2* in macaques were separately clustered, but both rhesus and cynomolgus alleles were found in the same cluster. Quite interestingly, *ULBP2.2* of macaques including olive baboon *ULBP2* and rhesus *ULBP5* appeared to be diverged from an ancestral *ULBP2.1*. In addition, *ULBP2* sequences from human, gorilla and chimpanzee as well as *ULBP5* and *ULBP6* sequences from human were clustered as a branch of *ULBP2.1* (Fig. 1). Furthermore, when other *ULBP* genes, *ULBP1*, *ULBP3*, and *ULBP4*, were included in the phylogenetic analysis, these genes were also clustered as

another branch of *ULBP2.1*, implying that these genes were diverged from the ancestral *ULBP2* in the primates (Supplementary Figure S1).

Diversity of *ULBP2* genes in the Old World Monkey

As for the diversity of *ULBP2* in macaques, non-synonymous substitutions were found at 14 sites in *Mamu-ULBP2.1*, 10 sites in *Mafa-ULBP2.1*, 15 sites in *Mamu-ULBP2.2*, and 16 sites in *Mafa-ULBP2.2* (Table 2). Amino acid sequences were deduced from the nucleotide sequences and alignment of the ULBP2 alleles showed that the ULBP2/RAET1H molecules in rhesus and cynomolgus macaques were homologous by more than 90 % to the human ULBP2 molecule in the α1 and α2 domains (Fig. 2). Among the polymorphic amino acid residues, six and eight residues in the ULBP2.1 and ULBP2.2 molecules, respectively, were observed in both rhesus and cynomolgus macaques (Fig. 2).

To investigate a possible role of the polymorphic residues, we created 3D structure models for ULBP2 molecules by referring the crystallographic data for human ULBP3 in complex with NKG2D, where ULBP2 residues at positions 22, 23, 70, 73, 77, 80, 83, 94, 165, 169, 170, and 172 composed of interacting surface with NKG2D (Supplementary Figure S2). It was found that three polymorphic residues at positions 73, 177, and 181 of rhesus ULBP2.1 were on the upper surface of α helix structures and pointed to the NKG2D receptor (Fig. 3a). Interestingly, the residue at position 73 could be a contacts site with Ser195 of NKG2D receptor, as deduced from the equivalent structure of human ULBP3. In contrast, none of the polymorphic residues were mapped on the surface of α helix structures in cynomolgus ULBP2.1 (Supplementary Figure S3).

On the other hand, two polymorphic residues at positions 158 and 181 of cynomolgus ULBP2.2 were on the upper surface of the α helix structure, while another polymorphic residue at position 172 was a possible interface site with Glu183 and Met184 of NKG2D in the equivalent human ULBP3, although it was not pointed up on the α helix of ULBP (Fig. 3b). In clear contrast and quite interestingly, none of the polymorphic residues were mapped on the surface of α helix in rhesus ULBP2.2 (Supplementary Figure S4). It should be noted here that the residue at position 20 is polymorphic in human ULBP2, while the residues at positions 80 and 172 are polymorphic in human ULBP6, indicating that both ULBP2 and ULBP6 might carry the allelic differences in the interaction with NKG2D in humans (Supplementary Figure S5).

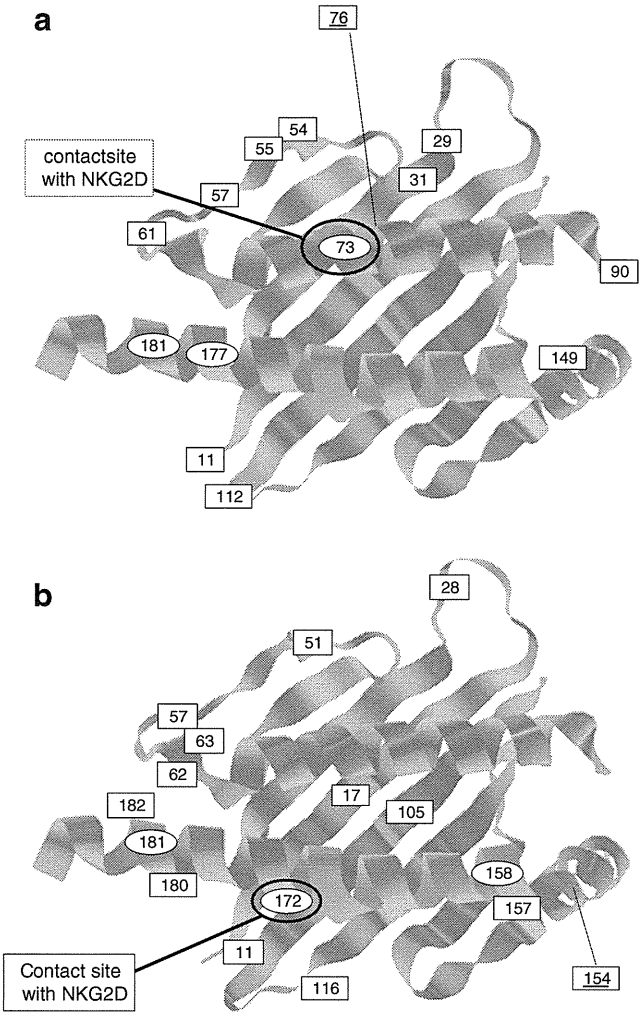

Fig. 3 Mapping of polymorphic sites on the 3D-structure model of macaque ULBP2 molecule. Polymorphic sites were mapped on the 3D structure model of ULBP2/RAET1H. Positions of polymorphic amino acid resides in the rhesus ULBP2.1 molecule (**a**) and cynomolgus ULBP2.2 molecule (**b**). Residues on the upper side of α helix are indicated by *circles*, while those on the outer side or on the β seat are indicated by *squares*. The residues mapped behind or beneath the α helix are underlined and represented by *dotted lines*. Possible contact sites with NKG2D (Radaev et al. 2001) are indicated

Discussion

In this study, we investigated the polymorphic nature of *ULBP2/RAET1H* in the Old World monkey. We previously reported that each member of the *ULBP/RAET1* gene family, except for *ULBP6/RAET1L*, was duplicated in the rhesus genome (Naruse et al., 2011). As expected, we obtained *ULBP2.1* and *ULBP2.2* sequences from both rhesus and cynomolgus macaques. On the other hand, any orthologous genes to human *ULBP6* were not detected in the macaques, even though *ULBP6* showed 96 % homology to *ULBP2* in humans (Radosavljevic et al. 2001). It was considered that *ULBP2.1* or *ULBP2.2* might be orthologous to human *ULBP6*. However, our phylogenetic analysis indicated that both human *ULBP2* and *ULBP6* were clustered with *ULBP2*s from chimpanzee and gorilla, as a branch of *ULBP2.1*. In addition, intron 2 sequences of ULBP2.2 in

macaques were relatively well conserved among *ULBP2*s from olive baboon, chimpanzee, western gorilla, and human as well as in human *ULBP6* than exon sequences. Furthermore, a Blast search showed that there was no *ULBP6*-like sequence in the genomes of chimpanzee and gorilla. These observations suggested that human *ULBP2* and *ULBP6* were diverged from an ancestral *ULBP2* after the diversification of human and other higher primates. The phylogenetic analysis also indicated that *ULBP2.2* might be diverged from *ULBP2.1* and the clustering of *ULBP2.1* alleles and *ULBP2.2* alleles did not depend on the species, supporting a trans-species evolution. Our observations were consistent with that ULBP/REAT molecule of placental mammals was originally diverged and duplicated in each species after an emigration from the *MHC* region (Kondo et al. 2010).

On the other hand, *Mafa-ULBP2.1*5* was placed at the diverging point of *ULBP2.2* in the phylogenetic tree (Fig. 1 and Supplementary Figure S1). As shown in Fig. 2, among the *ULBP2.1* alleles, only the *Mafa-ULBP2.1*5* has a replacement of Arg with Val at the position 105, which is a common feature of *Mamu-ULBP2.2* and *Mafa-ULBP2.2*. In addition, *Mafa-ULBP2.1*5* carries *ULBP2.2*-like sequences at the positions of 29 and 54. These characteristic features may eventually position the *Mafa-ULBP2.1*5* at the diverging point of *ULBP2.2*. Alternatively, gene conversion-like events from *ULBP2.2* had occurred in *ULBP2.1* to generate the *Mafa-ULBP2.1*5*.

In the present study, we denoted 15 and 11 *ULBP2.1* alleles and 11 and 10 *ULBP2.2* alleles in rhesus and cynomolgus macaques, respectively, of which more than 70 % of polymorphisms were non-synonymous. Induced expression of human ULBP2 molecule is involved in the recognition of virus-infected cell by NKG2D (Ward et al. 2009), although the functional significance of the polymorphisms in the extracellular domain of ULBP2 molecules remains to be deciphered. We demonstrated that several polymorphisms of ULBP2 molecules were located at the presumed contact sites with NKG2D or on the upper surface of α helix, which might have functional impacts. On the other hand, it has been reported that the sequence identities are less than 60 % among the ULBP molecules, while those between the ULBP and MIC molecules are about 25 % (Cosman et al. 2001). The interface residues appeared to be less conserved than the overall sequence among the ULBP molecules, and it was predicted that NKG2D could recognize the diversities of ULBP1 and ULBP2 molecules through induced-fit mechanisms in a similar manner as that of ULBP3 (Radaev et al. 2001). However, other previous studies revealed that the structural differences among the α2 domains of ULBP and MIC molecules affect the binding affinity to NKG2D and UL16, respectively (Wittenbrink et al. 2009; Spreu et al. 2006), suggesting that the ULBP polymorphisms demonstrated in this study might influence the efficacy of recognition by NKG2D. The functional impact of the polymorphisms should be investigated in future studies to decipher the evolutional and biological significance of the ULBP2 polymorphisms in the Old World monkeys.

Acknowledgments We thank Yukiko Ueda, Yasuko Saida, and Nana Ohkubo for their technical assistances. This work was supported in part by research grants from the Ministry of Health, Labor and Welfare, Japan and a Grant-in-Aid for scientific research from the Ministry of Education, Culture, Sports, Science, and Technology (MEXT), Japan. This work was also supported by a supporting program for women researchers from the Tokyo Medical and Dental University.

References

Antoun A, Jobson S, Cook M, O'Callaghan CA, Moss P, Briggs DC (2010) Single nucleotide polymorphism analysis of the NKG2D ligand cluster on the long arm of chromosome 6: extensive polymorphisms and evidence of diversity between human populations. Hum Immunol 71:610–620

Bacon L, Eagle RA, Meyer M, Easom N, Young NT, Trowsdale J (2004) Two human ULBP/RAET1 molecules with transmembrane region are ligands for NKG2D. J Immunol 173:1078–1084

Bauer S, Groh V, Wu J, Steinle A, Phillips JH, Lanier LL, Spies T (1999) Activation of NK cells and T cells by NKG2D, a receptor for stress-inducible MICA. Science 285:727–729

Chalupny NJ, Sutherland CL, Lawrence WA, Rein-Weston A, Cosman D (2003) ULBP 4 is a novel ligand for human NKG2D. Biochem Biophys Res Commun 305:129–135

Cosman D, Mullberg J, Sutherland CL, Chin W, Armitage R, Fanslow R, Kubin M, Chalupny NJ (2001) ULBPs, novel MHC class I-related molecules, bind to CMV glycoprotein UL16 and stimulate NK cytotoxicity through the NKG2D receptor. Immunity 14:123–133

Eagle RA, Traherne JA, Ashiru O, Wills MR, Trowsdale J (2006) Regulation of NKG2D ligand gene expression. Hum Immunol 67: 1159–1169

Eagle RA, Flack G, Warford A, Martinez-Borra J, Jafferji I, Traherne JA, Ohashi M, Boyle LH, Barrow AD, Caillat-Zucman S, Young NT, Trowsdale J (2009a) Celllar expression, trafficking, and function of two isoforms of human ULBP5/RAET1G. PLoS ONE 4:e4503

Eagle RA, Traherne JA, Hair JR, Jafferji I, Trowsdale J (2009b) ULBP6/RAET1L is an additional human NKG2D ligand. Eur J Immunol 39: 3207–3216

Gibbs RA, Rogers J, Katze MG et al (2007) Evolutionary and biomedical insights from the rhesus macaque genome. Science 316:222–234

Kondo M, Maruoka T, Otsuka N, Kasamatsu J, Fugo K, Hanzawa N, Kasahara M (2010) Comparative genomic analysis of mammalian NKG2D ligand family genes provides insights into their origin and evolution. Immunogenetics 62:441–450

Kulski JK, Anzai T, Shiina T, Inoko H (2004) Rhesus macaque class I duplicon structures, organization, and evolution within the alpha block of the major histocompatibility complex. Mol Biol Evol 21: 2079–2091

Matusali G, Tchigjou HK, Pontrelli G, Bernardi S, D'Ettorre G, Vullo V, Buonomini AR, Andreoni M, Santoni A, Cerboni C, Doria M (2013) Soluble ligands for the NKG2D receptor are released during HIV-1 infection and impair NKG2D expression and cytotoxicity of NK cells. FASEB J 27:2440–2450

Naruse TK, Chen Z, Yanagida R, Yamashita T, Saito Y, Mori K, Akari H, Yasutomi Y, Miyazawa M, Matano T, Kimura A (2010) Diversity of MHC class I genes in Burmese-origin rhesus macaque. Immunogenetics 62:601–611

Naruse TK, Okuda Y, Mori K, Akari H, Matano T, Kimura A (2011) ULBP4/RAET1E is highly polymorphic in the Old World Monkey. Immunogenetics 63:501–509

Otting N, Otting N, de Vos-Rouweler AJM, Heijmans CMC, de Groot NG, Doxiadis GGM, Bontrop RE (2007) MHC class I A region diversity and polymorphism in macaque species. Immunogentics 59:367–375

Pappworth IY, Wang EC, Rowe M (2007) The switch from latent to productive infection in Epstein-Barr virus-infected B cell is associated with sensitization to NK cell killing. J Virol 81:474–482

Pende D, Rivera P, Marcenaro S, Chang CC, Biassoni R, Conte R, Kubin M, Cosman D, Ferrone S, Moretta L, Moretta A (2002) Major histocompatibility complex class I-related chain A and UL16-binding protein expression on tumor cell lines of different histotypes: analysis of tumor susceptibility to NKG2D-dependent natural killer cell cytotoxicity. Cancer Res 62:6178–6186

Radaev S, Rostro B, Brooks AG, Colonna M, Sun PD (2001) Conformational plasticity revealed by the cocrystal structure of NKG2D and its class I MHC-like ligand ULBP3. Immunity 5: 1039–1049

Radosavljevic M, Cuillerier B, Wilson MJ, Clement O, Wicker S, Gilfillan S, Beck S, Trowsdale J, Bahram S (2001) A cluster of ten novel MHC class I related genes on human chromosome 6q24.2-q25.3. Genomics 79:114–123

Raulet DH (2003) Roles of the NKG2D immunoreceptor and its ligands. Nat Rev Immunol 3:781–790

Richard J, Phan TNQ, Ishizuka Y, Cohen EA (2013) Viral protein R upregulates expression of ULBP2 on uninfected bystander cells during HIV-1 infection of primary CD4+ T lymphocytes. Virology 443:248–256

Romphruk AV, Romphruk A, Naruse TK, Raroengjai S, Puapairoj C, Inoko H, Leelayuwat C (2009) Polymorphisms of NKG2Dligands: Diverse RAET1/ULBP genes in northeastern Thais. Immunogenetics 61:611–617

Saito Y, Naruse TK, Akari H, Matano T, Kimura A (2012) Diversity of MHC class I haplotypes in cynomolgus macaques. Immunogenetics 64:131–141

Spreu J, Stehle T, Steinle A (2006) Human cytomegalovirus-encoded UL16 discriminates MIC molecules by their α2 domains. J Immunol 177:3143–3149

Ward J, Bonaparte M, Sacks J, Guterman J, Fogli M, Mavilio D, Barker E (2007) HIV modulates the expression of ligands important in triggering natural killer cell cytotoxic responses on infected primary T-cell blasts. Blood 110:1207–1214

Ward J, Davis Z, DeHart J, Zimmerman E, Bosque A, Brunette E, Mavilio D, Placeless V, Barker E (2009) HIV-1 PR triggers natural killer cell-mediated lysis of infected cells through activation of the ATR-mediated DNA damage response. PLoS Pathogen 5:e1000613

Wittenbrink M, Spreu J, Steinle A (2009) Differential NKG2D binding to highly related human NKG2D ligands ULBP2 and RAET1G is determined by a single amino acid in the α2 domain. Eur J Immunol 39:1642–1651

Wu J, Song Y, Bakker ABH, Bauer S, Spies T, Lanier LL, Phillips JH (1999) An activating immunoreceptor complex formed by NKG2D and DAP 10. Science 285:730–732

Primates (2014) 55:441–445
DOI 10.1007/s10329-014-0421-7

ORIGINAL ARTICLE

Seroprevalence of Japanese encephalitis virus infection in captive Japanese macaques (*Macaca fuscata*)

Hiroshi Shimoda · Akatsuki Saito · Keita Noguchi · Yutaka Terada · Ryusei Kuwata · Hirofumi Akari · Tomohiko Takasaki · Ken Maeda

Received: 15 December 2013 / Accepted: 2 April 2014 / Published online: 19 April 2014

Abstract Japanese encephalitis virus (JEV), which is transmitted by mosquitoes, infects many animal species and causes serious acute encephalitis in humans and horses. In this study, a serosurvey of JEV in Japanese macaques (*Macaca fuscata*) reared in Aichi Prefecture was conducted using purified JEV as an antigen for ELISA. The results revealed that 146 of 332 monkeys (44 %) were seropositive for JEV. In addition, 35 of 131 monkeys (27 %) born in the facility were seropositive, and the annual infection rate in the facility was estimated as 13 %. Our results provide evidence of the frequent exposure of many Japanese macaques to JEV, suggesting that there is a risk of JEV transmission to humans by mosquitoes.

Keywords ELISA · Japanese encephalitis virus · *Macaca fuscata* · Monkeys

H. Shimoda · K. Noguchi · Y. Terada · R. Kuwata · K. Maeda (✉)
Laboratory of Veterinary Microbiology, Joint Faculty of Veterinary Medicine, Yamaguchi University, 1677-1 Yoshida, Yamaguchi, Yamaguchi 753-8515, Japan
e-mail: kmaeda@yamaguchi-u.ac.jp

A. Saito · H. Akari
Center for Human Evolution Modeling Research, Primate Research Institute, Kyoto University, 41-2 Kanrin, Inuyama, Aichi 484-8506, Japan

T. Takasaki
Division 2, Department of Virology 1, National Institute of Infectious Diseases, 1-23-1 Toyama, Shinjyuku, Tokyo 162-8640, Japan

Introduction

Japanese encephalitis virus (JEV) belongs to the genus *Flavivirus* and family *Flaviviridae*. JEV is transmitted primarily by mosquitoes (*Culex tritaeniorhynchus*), and pigs play a major role as amplifiers of JEV. The virus is widely endemic in Southeast Asia and the Western Pacific region, including Japan (Mackenzie et al. 2001); the annual number of cases of and deaths from Japanese encephalitis (JE) have reached approximately 50,000 and 10,000, respectively, in humans (Erlanger et al. 2009).

Although there were several thousand patients with JE in the 1950s in Japan, the incidence of JE decreased dramatically in the 1980s due to the introduction of a vaccination program in 1967 (Oya and Kurane 2007). In the last 20 years, <10 cases of JE have occurred annually, with most cases arising in western Japan, particularly the Kyushu district (Arai et al. 2008).

Although only a few cases of human JE occurred in Japan in the last two decades, an annual serological survey of JEV in pigs revealed that the virus was endemic, particularly in western Japan (Arai et al. 2008). In addition, various wild and domestic mammals, including wild boars, raccoons, raccoon dogs, and dogs, were seropositive for JEV (Hamano et al. 2007; Nidaira et al. 2007; Ohno et al. 2009; Shimoda et al. 2010). Therefore, there is still a high risk of JEV infection in various mammals in Japan, particularly in western Japan.

The seroprevalence of JEV among various species of monkeys has been examined previously. Cynomolgus monkeys (*Macaca fascicularis*), Japanese macaques (*Macaca fuscata*), green monkeys (*Chlorocebus sabaeus*), and pig-tailed macaques (*Macaca nemestrina*) were seropositive for JEV in several Asian countries (Yamane 1974; Yuwono et al. 1984; Inoue et al. 2003; Nakgoi et al. 2014).

In contrast, there was no evidence of JEV infection in toque macaques (*Macaca sinica*) in Sri Lanka, where JEV was endemic (Peiris et al. 1993). Although there are reports of JEV infection in various monkey species in Asia, the recent prevalence of the virus in Japan remains unknown. Therefore, an assessment of the prevalence of JEV in monkeys in Japan will provide information about the potential risk of transmission of JEV to humans.

In this study, we performed a serological survey of JEV infection among Japanese macaques using ELISA, and assessed the current risk of JEV infection in monkeys and humans in Japan.

Methods

Cells

Vero cells (JCRB number JCRB9013) derived from an African green monkey were purchased from the Health Science Research Resources Bank (HSRRB, Tokyo, Japan). Vero cells were cultured at 37 °C in 5 % CO_2 in Eagle's minimum essential medium (EMEM; GIBCO, Grand Island, NY, USA) supplemented with 5 % heat-inactivated fetal calf serum (FCS; J R Scientific, Woodland, CA, USA), 1 mM sodium pyruvate, 100 U/ml penicillin, and 100 μg/ml streptomycin (GIBCO). Mosquito-derived C6/36 cells (JCRB number IFO 50010) were cultured at 28 °C in 5 % CO_2 and Dulbecco's modified Eagle's medium (DMEM; GIBCO) supplemented with 10 % heat-inactivated FCS, 100 U/ml penicillin, and 100 μg/ml streptomycin.

Virus

JEV/sw/Chiba/88/2002 was originally isolated from the serum of a healthy pig in 2002, and has been genetically classified into genotype I (Nerome et al. 2007). The virus was propagated in C6/36 cells grown at 28 °C in DMEM supplemented with 2 % FCS and stored at −80 °C until use.

Monkey serum samples

A total of 332 Japanese macaques (*Macaca fuscata*) housed at the Primate Research Institute (PRI), Kyoto University in Aichi Prefecture, Japan were the subjects in this study, and serum samples were collected between October 2011 and February 2012. Among them, 131 monkeys were born at PRI. All monkeys examined in this study were bred in an environment where they have a possibility of frequently being bitten by mosquitoes. These experiments were conducted according to the rules of Kyoto University and guidelines for experimental animal welfare. Blood was collected from these monkeys under ketamine hydrochloride anesthesia. All sera used for virus neutralization test and ELISA were stored at −20 °C until use.

Virus neutralization test

To determine the presence of virus-neutralizing antibodies against JEV, an 80 % plaque reduction virus neutralization test was performed as described previously (Ohno et al. 2009; Shimoda et al. 2010, 2011). In brief, sera were diluted 1:5 in EMEM containing 2 % FCS. The diluted sera or medium alone were/was mixed with equal volumes of virus solution containing 100 PFUs of JEV/sw/Chiba/88/2002, and the mixtures were incubated at 37 °C for 90 min. After incubation, the mixtures were inoculated onto subconfluent Vero cells and incubated at 37 °C for 90 min. After washing twice with EMEM, the cells were overlaid with 0.8 % agarose (Lonza, Rockland, ME, USA) in EMEM containing 5 % FCS. After 4 days of incubation at 37 °C in 5 % CO_2, the cells were fixed with 10 % buffered formaldehyde for 1 h, and the agarose layer was removed. After staining with crystal violet, plaques were counted. Sera that reduced the number of plaques by more than 80 % in comparison with the mean number of plaques in control wells were considered to be JEV antibody-positive.

ELISA

An indirect ELISA using inactivated JEV originating from the Beijing 01 strain as the antigen was used to determine the seroprevalence of JEV in monkeys. This virus strain was propagated in Vero cells, and the virions were inactivated with formaldehyde and purified by ultracentrifugation. The inactivated JEV virions were diluted with adsorption buffer (0.05 M carbonate–bicarbonate buffer, pH 9.6) to a concentration of 5 μg/ml and distributed at 100 μl per well into 96-well microplates (Maxisorp; Nunc, Roskilde, Denmark). Negative control wells received an equivalent volume of adsorption buffer without antigen. After incubation at 37 °C for 2 h, plates were placed at 4 °C overnight. The wells were washed three times with phosphate-buffered saline (PBS) containing 0.05 % Tween 20 (PBS-T) and then incubated with 100 μl per well of 1 % Block Ace (Dainippon Pharmaceutical, Osaka, Japan) in PBS at 37 °C for 30 min. Test sera were diluted with PBS-T containing 0.4 % Block Ace. Wells were washed three times with PBS-T, 100 μl of diluted sera were added to duplicate wells, and plates were incubated at 37 °C for 30 min. Next, the wells were washed three times with PBS-T and incubated with 100 μl per well of Peroxidase Conjugated Purified Recomb® Protein A/G (Thermo Fisher Scientific, Rockford, IL, USA) diluted in PBS-T containing

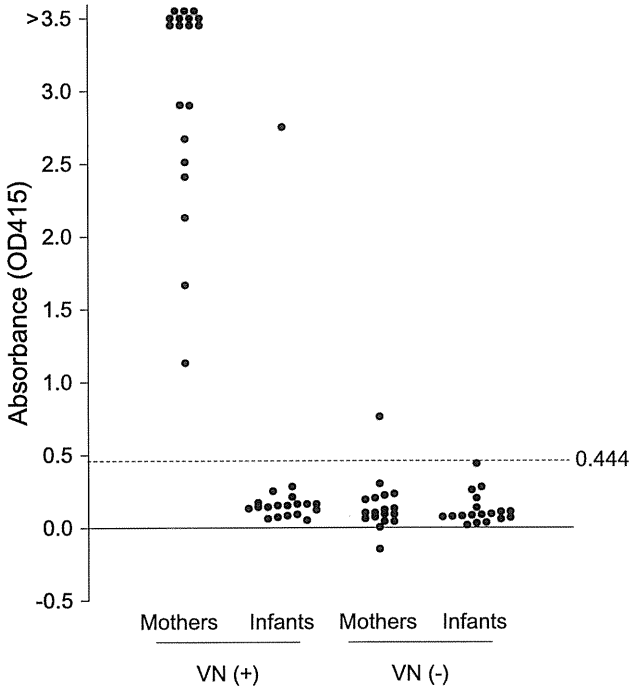

Fig. 1 ELISA values for JEV in infant Japanese macaques and their mothers. The lanes *VN (+)* and *VN (−)* denote positivity and negativity for JEV-neutralizing antibodies in the mothers, respectively. Infant monkeys that were born after the last summer to JEV-negative mothers according to the virus neutralization test were assumed to be JEV-negative when determining the cutoff value

0.4 % Block Ace at 37 °C for 30 min. Following three washes with PBS-T, 100 µl of horseradish peroxidase (Bio-Rad, Hercules, CA, USA) were added to each well. After incubation at room temperature for 30 min, the enzymatic reaction was stopped by adding 100 µl of 2 % oxalic acid to each well. The absorbance was measured by a spectrophotometer (Bio-Rad) with a 415-nm filter. All results were subtracted from the value of the non-antigen control.

Statistical analysis

To statistically analyze the results, the chi-squared test was performed. P values of <0.05 were considered statistically significant.

Results

Determination of the cutoff value

To determine the cutoff value, samples from 18 monkeys that were born after the last summer and had not yet experienced summer, and the mothers of which were confirmed as JEV-negative by the virus neutralization test, were examined by ELISA. The absorbance values obtained for these specimens ranged from 0.015 to 0.439, and the mean absorbance value was 0.123 with a standard deviation (SD) of 0.107 (Fig. 1). The mean value plus 3 × SD (a value of 0.444) was selected as the cutoff value between positive and negative results in this study. Only one monkey with a JEV-positive mother in virus neutralization testing was identified as JEV-positive by ELISA (Fig. 1). Because this baby monkey was 3 months old before the seasonal circulation of JEV, the detected antibodies are more likely to be of maternal origin.

Table 1 Seroprevalence of JEV in Japanese macaques born in Japan and reared in Aichi Prefecture, Japan

	Sex		Age (years)			Total
	Male	Female	0–3	4–7	≥8	
No. of monkeys examined	111	221	105	73	154	332
No. of positive monkeys	48	98	13	28	105	146
% of positive monkeys	43	44	12	38	68	44

Table 2 Seroprevalence of JEV in Japanese macaques born and reared in the same facility in Aichi Prefecture, Japan

	Sex		Age (years)			Total
	Male	Female	0–3	4–7	≥8	
No. of monkeys examined	63	68	93	18	20	131
No. of positive monkeys	17	18	13	8	14	35
% of positive monkeys	27	26	14	44	70	27
Annual positive rate in %[a]	15	12	–	–	–	13

[a] Annual positive rate was calculated according to the assumption that antibodies against JEV are maintained in Japanese macaques throughout their lives

Seroprevalence of JEV among monkeys in Japan

The results from the ELISA revealed that 146 of 332 monkeys (44 %) were seropositive for JEV. The seroprevalence among older monkeys (>7 years old, 68 %) was significantly higher than that among younger monkeys (0–3 years old, 12 %) ($P < 0.05$). There was no significant difference in seroprevalence between males (43 %) and females (44 %) (Table 1).

JEV infection in monkeys born and raised in Aichi Prefecture, Japan

To determine the annual seroprevalence among monkeys in Japan, we focused on monkeys born and raised in the same facility in Aichi Prefecture. The results illustrated that 35 of 131 monkeys (27 %) were seropositive for JEV (Table 2). The seroprevalence of JEV increased with age in

these monkeys, which was consistent with the results from other monkeys in Japan. The annual seroprevalence was calculated according to the assumption that JEV antibodies are maintained in Japanese macaques throughout their lives. As a result, approximately 13 % of monkeys were infected annually with JEV in Aichi Prefecture (Table 2).

Discussion

The ELISA performed in this study was previously established for JEV surveillance among dogs in Thailand (Shimoda et al. 2013). We adapted the method for surveillance in monkeys using protein A/G as a secondary antibody, and the results of the ELISA were correlated with those of the virus neutralization test (Fig. 1). Therefore, this method can be used for surveillance in monkeys as well as dogs. Furthermore, protein A/G is reported to have a broad binding ability for various mammalian immunoglobulins, including those of monkeys, deer, wild boars, and raccoon dogs (Inoshima et al. 1999), suggesting that it can be used for JEV surveillance in many species of wild mammals.

Serosurveys indicated that the risk of JEV infection is higher in western Japan than in eastern or northern areas (Arai et al. 2008; Shimoda et al. 2010). In this study, 27 % of monkeys in Aichi Prefecture, which is located in central Japan, were seropositive for JEV. Therefore, there may be a higher risk of JEV infection in monkeys in western Japan, including the Kyushu and Shikoku districts. One older serological study (before 1980) of the prevalence of JEV in 34 Japanese macaques bred in Aichi Prefecture indicated that 29.7 % of the animals were seropositive (Yuwono et al. 1984). In this study, 27 % of Japanese macaques born in the same facility were seropositive for JEV. Therefore, the prevalence of JEV among monkeys appears to have been maintained since the 1980s. In addition, many JEV-seropositive macaques will be protected from diseases associated with JEV, but not from JEV infection, as humans vaccinated with inactivated JEV vaccines developed NS1 antibodies due to natural JEV infection without any severe symptoms (Konishi and Suzuki 2002; Matsunaga et al. 2008).

To estimate the lowest annual seroprevalence of JEV, it was assumed that antibodies against JEV are maintained in Japanese macaques throughout the lives of the animals. However, the duration of human antibodies to JEV NS1 was estimated as 4.2 years (Konishi and Kitai 2009). Another study on JEV vaccination indicated that 18, 47, 82, and 100 % of humans would become virus neutralization antibody-negative at 5, 10, 15, and 20 years, respectively, after the second series of routine vaccinations (Abe et al. 2007). In experimentally JEV-infected dogs, virus neutralization titers increased until 21–28 days after infection, whereas they had slightly decreased 70 days after infection (Shimoda et al. 2011). These reports indicated that JEV antibodies are maintained for a long time but not throughout life. Therefore, the annual seroprevalence of JEV infection must be much higher than 13 %.

In this study, the seroprevalence of JEV increased with the age of the monkeys. This result appears to be correlated with the period of exposure to JEV-infected mosquitoes. Although there are no available data on the feeding pattern of *Culex tritaeniorhynchus*, the primary vector of JEV on humans and non-human primates, some other mosquito species, such as *Aedes* and *Haemagogus* species, display a similar feeding pattern between human and non-human primates (Marassa et al. 2009). Therefore, humans, similarly to Japanese macaques, will be bitten by JEV-infected mosquitoes around this facility.

In conclusion, because many Japanese macaques developed and maintained antibodies to JEV, there is a risk of JEV transmission to humans by JEV-carrying mosquitoes around this facility. In addition, because the prevalence of JEV among monkeys in Japan has not changed over the last 30 years, continuous surveillance for JEV infection and vaccination against JEV in Japan are required.

Acknowledgments This work was supported by a Grant-in-Aid for a Japan Society for the Promotion of Science Fellowship and a grant from the Ministry of Health, Labour, and Welfare of Japan (H20-Shinko-Ippan-003).

References

Abe M, Okada K, Hayashida K, Matsuo F, Shiosaki K, Miyazaki C, Ueda K, Kino Y (2007) Duration of neutralizing antibody titer after Japanese encephalitis vaccination. Microbiol Immunol 51:609–616

Arai S, Matsunaga Y, Takasaki T, Tanaka-Taya K, Taniguchi K, Okabe N, Kurane I, Vaccine Preventable Diseases Surveillance Program of Japan (2008) Japanese encephalitis: surveillance and elimination effort in Japan from 1982 to 2004. Jpn J Infect Dis 61:333–338

Erlanger TE, Weiss S, Keiser J, Utzinger J, Wiedenmayer K (2009) Past, present, and future of Japanese encephalitis. Emerg Infect Dis 15:1–7

Hamano M, Lim CK, Takagi H, Sawabe K, Kuwayama M, Kishi N, Kurane I, Takasaki T (2007) Detection of antibodies to Japanese encephalitis virus in the wild boars in Hiroshima prefecture, Japan. Epidemiol Infect 135:974–977

Inoshima Y, Shimizu S, Minamoto N, Hirai K, Sentsui H (1999) Use of protein AG in an enzyme-linked immunosorbent assay for screening for antibodies against parapoxvirus in wild animals in Japan. Clin Diagn Lab Immunol 6:388–391

Inoue S, Morita K, Matias RR, Tuplano JV, Resuello RR, Candelario JR, Cruz DJ, Mapua CA, Hasebe F, Igarashi A, Natividad FF (2003) Distribution of three arbovirus antibodies among monkeys (*Macaca fascicularis*) in the Philippines. J Med Primatol 32:89–94

Konishi E, Kitai Y (2009) Detection by ELISA of antibodies to Japanese encephalitis virus nonstructural 1 protein induced in subclinically infected humans. Vaccine 27:7053–7058

Konishi E, Suzuki T (2002) Ratios of subclinical to clinical Japanese encephalitis (JE) virus infections in vaccinated populations: evaluation of an inactivated JE vaccine by comparing the ratios with those in unvaccinated populations. Vaccine 21:98–107

Mackenzie JS, Chua KB, Daniels PW, Eaton BT, Field HE, Hall RA, Halpin K, Johansen CA, Kirkland PD, Lam SK, McMinn P, Nisbet DJ, Paru R, Pyke AT, Ritchie SA, Siba P, Smith DW, Smith GA, van den Hurk AF, Wang LF, Williams DT (2001) Emerging viral diseases of Southeast Asia and the Western Pacific. Emerg Infect Dis 7:497–504

Marassa AM, Paula MB, Gomes AC (2009) Biotin-avidin sandwich ELISA with specific human isotypes IgG1 and IgG4 for culicidae mosquito blood meal identification from an epizootic yellow fever area in Brazil. J Venom Anim Toxins Incl Trop Dis 15:696–706

Matsunaga T, Shoda M, Konishi E (2008) Japanese encephalitis viral infection remains common in Japan. Pediatr Infect Dis J 27:769–770

Nakgoi K, Nitatpattana N, Wajjwalku W, Pongsopawijit P, Kaewchot S, Yoksan S, Siripolwat V, Souris M, Gonzalez JP (2014) Dengue, Japanese encephalitis and Chikungunya virus antibody prevalence among captive monkey (*Macaca nemestrina*) colonies of Northern Thailand. Am J Primatol 76:97–102

Nerome R, Tajima S, Takasaki T, Yoshida T, Kotaki A, Lim CK, Ito M, Sugiyama A, Yamauchi A, Yano T, Kameyama T, Morishita I, Kuwayama M, Ogawa T, Sahara K, Ikegaya A, Kanda M, Hosoya Y, Itokazu K, Onishi H, Chiya S, Yoshida Y, Tabei Y, Katsuki K, Tabata K, Harada S, Kurane I (2007) Molecular epidemiological analyses of Japanese encephalitis virus isolates from swine in Japan from 2002 to 2004. J Gen Virol 88:2762–2768

Nidaira M, Taira K, Itokazu K, Kudaka J, Nakamura M, Ohno A, Takasaki T (2007) Survey of the antibody against japanese encephalitis virus in Ryukyu wild boars (*Sus scrofa riukiuanus*) in Okinawa, Japan. Jpn J Infect Dis 60:309–311

Ohno Y, Sato H, Suzuki K, Yokoyama M, Uni S, Shibasaki T, Sashika M, Inokuma H, Kai K, Maeda K (2009) Detection of antibodies against Japanese encephalitis virus in raccoons, raccoon dogs and wild boars in Japan. J Vet Med Sci 71:1035–1039

Oya A, Kurane I (2007) Japanese encephalitis for a reference to international travelers. J Travel Med 14:259–268

Peiris JS, Dittus WP, Ratnayake CB (1993) Seroepidemiology of dengue and other arboviruses in a natural population of toque macaques (*Macaca sinica*) at Polonnaruwa, Sri Lanka. J Med Primatol 22:240–245

Shimoda H, Ohno Y, Mochizuki M, Iwata H, Okuda M, Maeda K (2010) Dogs as sentinels for human infection with Japanese encephalitis virus. Emerg Infect Dis 16:1137–1139

Shimoda H, Tamaru S, Morimoto M, Hayashi T, Shimojima M, Maeda K (2011) Experimental infection of Japanese encephalitis virus in dogs. J Vet Med Sci 73:1241–1242

Shimoda H, Inthong N, Noguchi K, Terada Y, Nagao Y, Shimojima M, Takasaki T, Rerkamnuaychoke W, Maeda K (2013) Development and application of an indirect enzyme-linked immunosorbent assay for serological survey of Japanese encephalitis virus infection in dogs. J Virol Methods 187:85–89

Yamane Y (1974) Natural virus infection in green and cynomolgus monkeys. Kitasato Arch Exp Med 47:15–66

Yuwono J, Suharyono W, Koiman I, Tsuchiya Y, Tagaya I (1984) Seroepidemiological survey on dengue and Japanese encephalitis virus infections in Asian monkeys. Southeast Asian J Trop Med Public Health 15:194–200

JVI Journals.ASM.org

Novel Permissive Cell Lines for Complete Propagation of Hepatitis C Virus

Mai Shiokawa,[a] Takasuke Fukuhara,[a] Chikako Ono,[a] Satomi Yamamoto,[a] Toru Okamoto,[a] Noriyuki Watanabe,[b] Takaji Wakita,[b] Yoshiharu Matsuura[a]

Department of Molecular Virology, Research Institute for Microbial Diseases, Osaka University, Osaka, Japan[a]; Department of Virology II, National Institute of Infectious Diseases, Tokyo, Japan[b]

ABSTRACT

Hepatitis C virus (HCV) is a major etiologic agent of chronic liver diseases. Although the HCV life cycle has been clarified by studying laboratory strains of HCV derived from the genotype 2a JFH-1 strain (cell culture-adapted HCV [HCVcc]), the mechanisms of particle formation have not been elucidated. Recently, we showed that exogenous expression of a liver-specific microRNA, miR-122, in nonhepatic cell lines facilitates efficient replication but not particle production of HCVcc, suggesting that liver-specific host factors are required for infectious particle formation. In this study, we screened human cancer cell lines for expression of the liver-specific α-fetoprotein by using a cDNA array database and identified liver-derived JHH-4 cells and stomach-derived FU97 cells, which express liver-specific host factors comparable to Huh7 cells. These cell lines permit not only replication of HCV RNA but also particle formation upon infection with HCVcc, suggesting that hepatic differentiation participates in the expression of liver-specific host factors required for HCV propagation. HCV inhibitors targeting host and viral factors exhibited different antiviral efficacies between Huh7 and FU97 cells. Furthermore, FU97 cells exhibited higher susceptibility for propagation of HCVcc derived from the JFH-2 strain than Huh7 cells. These results suggest that hepatic differentiation participates in the expression of liver-specific host factors required for complete propagation of HCV.

IMPORTANCE

Previous studies have shown that liver-specific host factors are required for efficient replication of HCV RNA and formation of infectious particles. In this study, we screened human cancer cell lines for expression of the liver-specific α-fetoprotein by using a cDNA array database and identified novel permissive cell lines for complete propagation of HCVcc without any artificial manipulation. In particular, gastric cancer-derived FU97 cells exhibited a much higher susceptibility to HCVcc/JFH-2 infection than observed in Huh7 cells, suggesting that FU97 cells would be useful for further investigation of the HCV life cycle, as well as the development of therapeutic agents for chronic hepatitis C.

More than 170 million individuals worldwide are infected with hepatitis C virus (HCV), and the cirrhosis and hepatocellular carcinoma induced by HCV infection are life-threatening diseases (1). Current standard therapy combining pegylated-interferon (peg-IFN) and ribavirin (RBV) has achieved a sustained virological response (SVR) in 50% of individuals infected with HCV genotype 1 (2). Recently, directly acting antiviral (DAA) agents have been applied in a clinical setting (3). An SVR rate of over 80% has been realized by combination therapy with peg-IFN, RBV, and NS3/4A inhibitors in genotype 1 patients (4, 5). In addition, several DAAs, including inhibitors for NS3/4A protease, NS5A, and NS5B polymerase, are currently in clinical trials. Several reports have shown that *in vitro* replication of HCV RNA is significantly inhibited by treatment with daclatasvir (NS5A inhibitor) and asunaprevir (NS3 protease inhibitor), and these two DAAs are also effective for patients infected with genotype 1 HCV who showed no response to previous therapy with peg–IFN-α and RBV (6–8). On the other hand, it has been shown that drug-resistant breakthrough viruses emerge during treatment with DAAs (9–12). Therefore, identification of host factors crucial for the propagation of HCV is an important task for the development of novel therapeutics for chronic hepatitis C with a low frequency of emergence of drug-resistant viruses.

The establishment of an *in vivo* infection model has been hampered by the narrow host range and tissue tropism of HCV. Although chimpanzees are the only experimental animals susceptible to HCV infection, it is difficult to use a chimpanzee model of experimental infection due to ethical concerns (13, 14). In addition, *in vitro* infection models have also been restricted to the combination of cell culture-adapted clones based on the genotype 2a JFH-1 strain (HCVcc) and human hepatoma cell lines, including Huh7 (15). Recently, several reports have shown that the exogenous expression of microRNA-122 (miR-122) facilitates the efficient propagation of HCVcc in HepG2 and Hep3B cells, which are nonpermissive for propagation of HCVcc (16, 17). Furthermore, we reported that nonhepatic cell lines, including Hec1B cells derived from uterine endometrial adenocarcinoma, also permit replication of HCV RNA by exogenous expression of miR-122 (18). These reports indicate that miR-122 is one of the most important determinants for liver tropism of HCV infection. Interestingly, formation of infectious particles was not observed in

Received 26 December 2013 Accepted 25 February 2014
Published ahead of print 5 March 2014
Editor: T. S. Dermody
Address correspondence to Yoshiharu Matsuura, matsuura@biken.osaka-u.ac.jp.

doi:10.1128/JVI.03839-13

spite of efficient replication of HCV RNA in nonhepatic cells, suggesting that liver-specific factors other than miR-122 are involved in HCV assembly. Previous reports suggested that very-low-density lipoprotein (VLDL)-associated proteins, including apolipoprotein B (ApoB), apolipoprotein E (ApoE), and microsomal triglyceride transfer protein (MTTP), play important roles in infectious particle production of HCV (19–23). In addition, Miyanari et al. indicated that lipid droplets (LDs) are crucial organelles for HCV particle assembly (24). These reports suggest that liver-specific lipid metabolism and liver-specific host factors closely participate in assembly of HCV.

Cancer cells are classified into well-differentiated and intermediately and poorly differentiated stages, and these stages have been shown to be strongly related to cancer behaviors, with an immature tumor generally being more aggressive than its more differentiated counterpart. Thus, it is believed that well-differentiated cancer cells maintain the tissue-specific cellular functions and exhibit morphology similar to that of normal cells (25). Permissive cell lines for HCV propagation, including Huh7, HepG2, and Hep3B cells, are derived from well-differentiated hepatocellular carcinoma (HCC) (26, 27). In addition, recent reports indicated that hepatocyte-like cells derived from induced pluripotent stem cells (iPS cells/iPSCs) express high levels of miR-122 and VLDL-associated proteins and support propagation of HCVcc (28–30). These results suggest that the hepatic differentiation required for hepatic functions is involved in HCV propagation.

In this study, we identified novel cell lines supporting complete propagation of HCVcc by screening cancer cell lines expressing α-fetoprotein (AFP), which is highly expressed in well-differentiated hepatocellular carcinoma and evaluated in most cancer cell lines (31). These cells exhibit high levels of expression of liver-specific host factors and permit complete propagation of HCVcc without any exogenous expression of liver-specific factors, including receptor molecules, miR-122, and apolipoproteins. Our current study suggests that hepatic differentiation participates in the expression of liver-specific host factors required for complete propagation of HCV.

MATERIALS AND METHODS

NextBio Body Atlas. The NextBio Body Atlas application allows the aggregated analysis of gene expression across various normal tissues, normal cell types, and cancer cell lines. It enables us to investigate the expression of individual genes as well as gene sets. Samples for Body Atlas data are obtained from publicly available studies that are internally curated, annotated, and processed (32). Body Atlas measurements are generated from all available RNA expression studies that used Affymetrix U133 Plus or U133A Genechip arrays for human studies. The results for 128 human tissue samples from 1,067 arrays, those for 157 human cell types from 1,474 arrays, and those for 359 human cancer cell lines from 376 arrays are incorporated. In this study, we screened cell lines expressing a high level of AFP. The details of the analysis protocol developed by NextBio were described previously (32). The raw data used in this application are derived from the GSK Cancer Cell Line data deposited at the National Cancer Institute website (https://array.nci.nih.gov/caarray/project/woost-00041).

Plasmids. The cDNA clones of pri-miR-122 and *Aequorea coerulescens* green fluorescent protein (AcGFP) were inserted between the XhoI and XbaI sites of lentiviral vector pCSII-EF-RfA, which was provided by M. Hijikata, and the resulting plasmids were designated pCSII-EF-miR-122 and pCSII-EF-AcGFP, respectively. Plasmids pHH-JFH1-E2p7NS2mt, encoding a cDNA of a full-length RNA of the JFH-1 strain, and pJFH2/AS/mtT4, encoding a cDNA of a full-length RNA of the JFH-2 strain, were described previously (33, 34). pSGR-Con1, which encodes a subgenomic replicon (SGR) of the Con1 strain, was provided by R. Bartenschlager. pIFN-β-Luc and pISRE-Luc carrying a firefly luciferase (Luc) gene under the control of the IFN-β- and IFN-sensitive response element (ISRE) promoters, respectively, were provided by S. Akira. The internal control plasmid encoding a *Renilla* luciferase (pRL-SV40) was purchased from Promega (Madison, WI). The plasmids used in this study were confirmed by sequencing with an ABI Prism 3130 genetic analyzer (Applied Biosystems, Tokyo, Japan).

Cell lines. All cell lines were cultured at 37°C under the conditions of a humidified atmosphere and 5% CO_2. Human hepatocellular carcinoma-derived Huh7, Hep3B, HepG2, and JHH-4 (JCRB0435) cells, embryonic kidney-derived 293T cells, gastric cancer-derived FU97 (JCRB1074) cells, and ovarian adenocarcinoma-derived OV-90 cells were maintained in Dulbecco's modified Eagle's medium (DMEM; Sigma-Aldrich, St. Louis, MO) supplemented with 100 U/ml penicillin, 100 μg/ml streptomycin, and 10% fetal calf serum (FCS). JHH-4 and FU97 cells were obtained from the Japanese Collection of Research Bioresources (JCRB) Cell Bank. OV-90 cells were obtained from the American Type Culture Collection (ATCC). 293T-CLDN cells stably expressing claudin-1 (CLDN1) were established by the introduction of expression plasmid pCAG-pm3 encoding CLDN1 under the control of the CAG promoter. The Huh7-derived cell line Huh7.5.1 was provided by F. Chisari. Huh7 and FU97 cells harboring the SGR of the Con1 strain (Con1-SGR) were prepared as described previously (35) and maintained in DMEM containing 1 mg/ml and 400 μg/ml of G418 (Nacalai Tesque, Kyoto, Japan), respectively.

Preparation of viruses. HCVs derived from the genotype 2a JFH-1 strain (HCVcc) were prepared after serial passages of the culture supernatants of Huh7.5.1 cells transfected with pHH-JFH1-E2p7NS2mt into Huh7.5.1 cells (33). HCVs derived from the genotype 2a JFH-2 strain (HCVcc/JFH-2) were prepared by several passages of the culture supernatants of Huh7.5.1 cells electroporated with JFH-2 RNA transcribed *in vitro*. Infectious titers were determined by a focus-forming assay and expressed as focus-forming units (FFU) (15). The vesicular stomatitis virus (VSV) variant NCP12.1 derived from the Indiana strain was provided by M. Whitt. Pseudotype VSVs bearing HCV E1 and E2 glycoproteins (HCVpv), were prepared as described previously (36), and infectivity was assessed by a luciferase assay system (Promega) according to a protocol provided by the manufacturer and expressed in relative light units (RLU).

Antibodies and drugs. Mouse monoclonal antibodies to HCV nonstructural protein 5A (NS5A) and β-actin were purchased from Austral Biologicals (San Ramon, CA) and Sigma-Aldrich, respectively. Rabbit anti-HCV core protein was prepared as described previously (37). Mouse anti-E2 polyclonal antibody was also prepared (unpublished data). Anti-human CD81 (hCD81) monoclonal antibody (JS-81) and rabbit anti-scavenger receptor class B type 1 (SR-BI) antibody were purchased from BD Biosciences (Franklin Lakes, NJ) and Novus Biologicals (Littleton, CO), respectively. Rabbit anti-CLDN1 and anti-occludin (OCLN) antibodies, Alexa Fluor 488 (AF488)-conjugated anti-rabbit and -mouse IgG antibodies, and AF594-conjugated anti-rabbit IgG antibodies were purchased from Life Technologies (Carlsbad, CA). Rabbit anti-signal transducer and activators of transcription 2 (STAT2) antibody and anti-calregulin antibody were purchased from Santa Cruz (Santa Cruz, CA). Rabbit anti-IFN regulatory factor 3 (IRF3) antibody was purchased from Abcam (Cambridge, United Kingdom). Phycoerythrin (PE)-conjugated anti-hCD81 and anti-mouse IgG antibodies were purchased from BD Biosciences. Anti-ApoB horseradish peroxidase (HRP)-conjugated antibody was purchased from ALerCHEK (Springvale, ME). The HCV NS3/4A protease inhibitor was purchased from Acme Bioscience (Salt Lake City, UT). Human recombinant alpha IFN (IFN-α) was purchased from PBL Biomedical Laboratories (Piscataway, NJ). BODIPY558/568 lipid probe and 4′, 6-diamidino-2-phenylindole (DAPI) were purchased from Life Technologies and Vector Laboratories, Inc. (Burlingame, CA), respectively. Cyclosporine and CP-346086 were purchased from Sigma-Aldrich. Ribavirin (RBV) was purchased from Tokyo Chemical Industry

(Tokyo, Japan). BMS-790052 and PSI-7977 were purchased from Shanghai Haoyuan Chemexpress (Shanghai, China). BMS-200150 was purchased from ChemStep (Martillac, France). The locked nucleic acid (LNA) targeted to miR-122, miR-122–LNA (5′-CcAttGTcaCaCtCC-3′), and its negative control, control-LNA (Ctrl-LNA) (5′-CcAttCTgaCcCtA C-3′), were purchased from Gene Design (Osaka, Japan); LNAs and DNAs are indicated in capital and lowercase letters, respectively. Sulfur atoms in oligonucleotide phosphorothioates are substituted for nonbridging oxygen atoms. The capital C indicates LNA methylcytosine.

Transfection and lentiviral gene transduction. Cells were transfected with the plasmids by using TransIT LT-1 transfection reagents (Mirus, Madison, WI) according to the manufacturer's protocol. LNAs were introduced into cells by Lipofectamine RNAi MAX (Life Technologies). The lentiviral vectors and ViraPower lentiviral packaging mix (Life Technologies) were cotransfected into 293T cells, and the supernatants were recovered at 48 h posttransfection. The lentivirus titer was determined by a lenti-XTM quantitative reverse transcription-PCR (qRT-PCR) titration kit (Clontech, Mountain View, CA), and the expression levels of miR-122 and AcGFP were determined at 48 h postinoculation.

Quantitative RT-PCR. HCV RNA levels were determined by a method described previously (38). Total RNA was extracted from cells by using an RNeasy minikit (Qiagen, Valencia, CA), and the first-strand cDNA synthesis and qRT-PCR were performed with TaqMan EZ RT-PCR core reagents and a ViiA7 system (Life Technologies), respectively, according to the manufacturer's protocol. The primers for TaqMan PCR targeted to the noncoding region of HCV RNA were synthesized as previously reported (39). To determine the expression of miR-122, total miRNAs were prepared by using an miReasy minikit (Qiagen), and miR-122 was determined by using the fully processed miR-122-specific RT and PCR primers provided in the TaqMan microRNA assays (Life Technologies) according to the manufacturer's protocol. U6 small nuclear RNA was used as an internal control. Fluorescent signals were analyzed with the ViiA7 system.

Immunoblotting. Cells were lysed on ice in lysis buffer (20 mM Tris-HCl [pH 7.4], 135 mM NaCl, 1% Triton X-100, 10% glycerol) supplemented with a protease inhibitor mix (Nacalai Tesque). Culture supernatants of cells incubated for 3 days were used for detection of ApoB. The samples were boiled in loading buffer and subjected to a 5% to 20% gradient SDS-PAGE or 3 to 8% Tris-acetate gel (Thermo Scientific, Waltham, MA). The proteins were transferred to polyvinylidene difluoride membranes (Millipore, Bedford, MA) and reacted with the appropriate antibodies. The immune complexes were visualized with SuperSignal West Femto substrate (Pierce, Rockford, IL) and detected with an LAS-3000 image analyzer system (Fujifilm, Tokyo, Japan).

Immunofluorescence assay. Cells cultured on glass slides were fixed with 4% paraformaldehyde (PFA) in phosphate-buffered saline (PBS) at room temperature for 30 min, permeabilized for 20 min at room temperature with PBS containing 0.2% Triton X-100, washed three times with PBS, and blocked with PBS containing 2% FCS for 1 h at room temperature. Then cells were incubated with PBS containing appropriate primary antibodies at room temperature for 1 h, washed three times with PBS, and incubated with PBS containing AF488- or AF594-conjugated secondary antibodies at room temperature for 45 min. For lipid droplet staining, cells were incubated in medium containing 20 μg/ml BODIPY for 20 min at 37°C, washed with prewarmed fresh medium, and incubated for 20 min at 37°C. The stained cells were covered with Vectashield Mounting Medium containing DAPI (Vector Laboratories Inc., Burlingame, CA) and observed with a FluoView FV1000 laser scanning confocal microscope (Olympus, Tokyo, Japan).

***In vitro* transcription, RNA transfection, and colony formation.** The plasmid pSGR-Con1 was linearized with ScaI and transcribed *in vitro* by using a MEGAscript T7 kit (Life Technologies) according to the manufacturer's protocol. The *in vitro*-transcribed RNA (10 μg) was electroporated into FU97 cells at 10^7 cells/0.4 ml under conditions of 210 V and 960 μF using a Gene Pulser apparatus (Bio-Rad, Hercules, CA) and plated on DMEM containing 10% FCS. The medium of FU97 cells was replaced with fresh DMEM containing 10% FCS and 400 μg/ml G418 at 24 h postelectroporation. The remaining colonies were cloned by using a cloning ring (Asahi Glass, Tokyo, Japan) or fixed with 4% PFA in PBS and stained with crystal violet at 5 weeks postelectroporation.

Flow cytometry. Cultured cells were detached with 0.25% trypsin-EDTA, incubated with PE-conjugated anti-hCD81 antibody or anti-mouse IgG antibody for 1 h at 4°C, washed twice with PBS containing 1% bovine serum albumin (BSA), and analyzed by using a flow cytometry system (FACSCalibur; BD Biosciences).

Gene silencing. A commercially available small interfering RNA (siRNA) pool targeting ApoB and ApoE (siGENOME SMARTpool human ApoB and ApoE) and a control nontargeting siRNA were purchased from Dharmacon (Buckinghamshire, United Kingdom) and transfected into JHH-4 and FU97 cells using Lipofectamine RNAi MAX (Life Technologies) according to the manufacturer's protocol.

Luciferase assay. Cells seeded onto 24-well plates at a concentration of 5×10^4 cells/well were transfected with 250 ng of each of the plasmids, stimulated with the appropriate ligands for 24 h at 24 h posttransfection, and lysed in 100 μl of passive lysis buffer (Promega). Luciferase activity was measured in 20-μl aliquots of the cell lysates using a dual-luciferase reporter assay system (Promega). Firefly luciferase activity was standardized with that of *Renilla* luciferase cotransfected with the internal control plasmid pRL-SV40 and was expressed in RLU.

Neutralization assay. Huh7, JHH-4, and FU97 cells were pretreated with 10 μg/ml of anti-hCD81 (JS-81) monoclonal antibody for 1 h at 37°C and then inoculated with HCVcc (1×10^6 FFU/ml). Anti-E2 monoclonal antibody (10 μg/ml) was incubated with HCVcc (1×10^6 FFU/ml) for 1 h and then inoculated into cells. Intracellular HCV RNA levels at 12, 24, 48, and 72 h postinfection were determined by qRT-PCR.

Buoyant density gradient analysis. Culture supernatants of Huh7.5.1 and FU97 cells infected with HCVcc at 72 h postinfection were passed through 0.45-μm-pore-size filters and concentrated by a Spin-X Concentrator (100,000-molecular-weight cutoff column; Corning, Lowell, MA). One milliliter of concentrated sample was layered onto the top of a linear gradient formed from 10% to 40% of OptiPrep (Axis-Shield PoC, Oslo, Norway) in PBS and spun at 32,000 rpm for 16 h at 4°C by using an SW41-Ti rotor (Beckman Coulter, Fullerton, CA). Each fraction collected from the top was analyzed by qRT-PCR, focus-forming assay, and immunoblotting.

Statistical analysis. The data for statistical analyses are the averages of three independent experiments. Results were expressed as the means ± standard deviations. The significance of differences in the means was determined by Student's *t* test.

RESULTS

JHH-4 and FU97 cells express high levels of the liver-specific host factors required for HCV propagation. AFP is known as a marker for not only well-differentiated HCC (31) but also the early stage of differentiation to hepatocytes in embryonic stem (ES)/iPS cells (29, 40, 41). Generally, well-differentiated cancer cells show better maintenance of their cell-specific functions than poorly differentiated cancer cells. Therefore, we hypothesized that cancer cell lines with high levels of AFP expression retain sufficient hepatic function for HCV propagation. To examine this hypothesis, we first screened cancer cell lines by using the NextBio Body Atlas application and identified the following cell lines that expressed high levels of AFP: Takigawa and FU97 cells derived from gastric cancer, HepG2 and Hep3B cells from hepatocellular carcinoma, Caco-2 cells from colon cancer, and OV-90 cells from ovarian cancer. To evaluate the correlation of AFP expression with the hepatic functions in these cell lines, we examined the expression of liver-specific host factors, including albumin (ALB), ApoB, and ApoE, by using the Web-based NextBio search engine and found

that these cell lines expressed higher levels of the liver-specific genes than the HEK293 cells used as negative controls (Fig. 1A). These results suggested that the expression of AFP was correlated with that of the examined liver-specific host factors in cancer cell lines. Next, to confirm this correlation, the expression levels of ALB, ApoB, ApoE, MTTP, and miR-122 were determined by qPCR in AFP-expressing cell lines, including FU97, OV-90, and HCC-derived Huh7, HepG2, Hep3B, and JHH-4 cells (Fig. 1B). Takigawa cells were difficult to culture, and Caco-2 cells have previously been reported to permit entry and replication of HCV (42, 43); therefore, we excluded these cell lines for further analyses. JHH-4 cells were previously shown to permit a partial propagation of HCV in a three-dimensional cultivation by using a radial-flow bioreactor system upon inoculation with plasma from an HCV carrier (44). In contrast to 293T cells, these AFP-expressing cell lines express high levels of the examined liver-specific host factors, suggesting that these cell lines maintain their hepatic functions. Because previous studies have shown that Huh7, HepG2, and Hep3B cells are susceptible to HCVcc infection, we selected JHH-4, FU97, and OV-90 cells for further investigation as new cell line candidates for HCV propagation. It is well known that hepatocytes and intestinal cells produce ApoB100 and ApoB48, respectively. ApoB100 was detected in the culture supernatants of Huh7, JHH-4, FU97, and OV-90 cells but not in those of 293T cells by immunoblotting (Fig. 1C). These results suggest that FU97 and OV-90 cells are differentiated into hepatocyte-like cells and possess liver-specific functions. The expression of entry receptor molecules for HCV, including hCD81, CLDN1, OCLN, and SR-BI (45–48), in these cell lines was confirmed by immunoblotting and fluorescence-activated cell sorting (FACS) analyses (Fig. 1D and E). To further determine the authenticity of the receptor candidates for HCV entry, HCVpv was inoculated into these cell lines. Although the infectivity of HCVpv to JHH-4 and FU97 cells was comparable to that in Huh7 cells, OV-90 cells did not show any susceptibility to HCVpv infection (Fig. 1F). Cell surface expression of CLDN1 and OCLN was detected in OV-90 cells (data not shown); therefore, lack of susceptibility of OV-90 cells to HCVpv infection might be attributable to lower expression of SR-B1 and hCD81 in OV-90 cells than in other cell lines (Fig. 1D and E). Thus, we selected JHH-4 and FU97 cells for further investigation of HCV propagation.

JHH-4 and FU97 cells permit HCV propagation. To examine the susceptibility of JHH-4 and FU97 cells to HCV propagation, HCVcc was inoculated into these cells at a multiplicity of infection (MOI) of 1, and intracellular HCV RNA and infectious titers in the culture supernatants were determined by qRT-PCR and focus-forming assay, respectively. FU97 cells exhibited higher levels of HCV gene expression than JHH-4 cells, and these levels increased continuously until 48 h postinfection; treatment with IFN-α significantly inhibited HCV gene expression in both JHH-4 and FU97 cells (Fig. 2A, left panels). In addition, substantial amounts of infectious particles were detected in the culture supernatants of JHH-4 and FU97 cells infected with HCVcc, in contrast to the lack of infectious particles in the culture supernatants of 293T-CLDN/miR-122 cells infected with HCVcc (Fig. 2A, bar graph). Recent reports have shown that exogenous expression of miR-122 enhances HCV RNA abundances in several hepatic or nonhepatic cell lines (16–18). Therefore, we examined the effect of miR-122 overexpression on HCV RNA abundances in both JHH-4 and FU97 cells. miR-122 was introduced in these cells by a lentiviral vector encoding pri-miR-122, an unprocessed miR-122, and miR-122 expression was confirmed by quantitative PCR (qPCR) analysis (Fig. 2B, bar graph). In contrast to the slight increase of HCV RNA in FU97 cells, JHH-4 cells exhibited a significant increase of HCV RNA, suggesting that the expression level of miR-122 is a key determinant for the efficient propagation of HCV (Fig. 2B, right panels). A previous study has shown that NS5A proteins were localized around the endoplasmic reticulum (ER) membrane, and accumulation of core protein around lipid droplets (LDs) facilitates efficient assembly of infectious particles in Huh7 cells (24). Immunofluorescence microscopy observation revealed that core and NS5A proteins in JHH-4 and FU97 cells infected with HCVcc were detected around LDs and in the ER together with double-stranded RNA (dsRNA), respectively (Fig. 2C). These results suggest that expression of liver-specific factors permits complete propagation of HCVcc in JHH-4 and FU97 cells and that hepatic characteristics play crucial roles in HCV propagation.

JHH-4 and FU97 cells permit complete propagation of HCVcc without any exogenous expression of host factors crucial for propagation of HCV. To further characterize the propagation of HCV in JHH-4 and FU97 cells, we examined the effects of the HCV inhibitors on the replication of HCV RNA. Preincubation with anti-HCV E2 antibody and pretreatment of cells with anti-hCD81 monoclonal antibody significantly inhibited HCVcc infection not only in Huh7 cells but also in JHH-4 and FU97 cells, suggesting that hCD81 is also involved in HCV entry into JHH-4 and FU97 cells (Fig. 3A, left panels). To examine the effect of miR-122 expression on HCV RNA abundances, cells were treated with LNA specific to either miR-122 (miR-122–LNA) or a nonspecific LNA (Ctrl-LNA) at 6 h before infection with HCVcc. Treatment with miR-122–LNA but not with Ctrl-LNA significantly reduced the HCV RNA abundances in these cell lines, suggesting that miR-122 also plays a crucial role in the efficient propagation of HCVcc in JHH-4 and FU97 cells (Fig. 3A, right panels). Previous reports showed that treatment with MTTP inhibitors inhibited the production of infectious particles of HCVcc in Huh7 cells (20, 22). Although intracellular HCV RNA levels in Huh7, JHH-4, and FU97 cells were not inhibited by the treatment with MTTP inhibitors, including CP-346086 and BMS-200150 (Fig. 3B, left panels), the production of infectious particles was significantly decreased in these cells (Fig. 3B, right panels). These results suggest that the VLDL secretion pathway also participates in the propagation of HCV in JHH-4 and FU97 cells. Furthermore, it was shown that ApoB and ApoE are involved in the production of HCV particles in Huh7 cells (20–22). To confirm the role of ApoB and ApoE in HCV propagation in JHH-4 and FU97 cells, the expression of ApoB and ApoE was suppressed by siRNAs (Fig. 3C, left panels). The suppression of ApoB and ApoE expression significantly reduced HCV RNA levels in cells infected with HCVcc at an MOI of 1 (Fig. 3C, middle panels) and significantly reduced the infectious titers in the supernatants (Fig. 3C, right panels) at 72 h postinfection. Collectively, these results suggest that the JHH-4 and FU97 cells permit complete propagation of HCVcc without any exogenous expression of the host factors crucial for propagation of HCV, including receptor molecules, miR-122, and VLDL-associated proteins. FU97 cells exhibited higher susceptibility to HCVcc propagation than JHH-4 cells (Fig. 2A), and thus we characterized the FU97 cells in greater detail.

Establishment of HCV RNA replicon and cured cells by using FU97 cells. To further examine the characteristics of FU97 cells

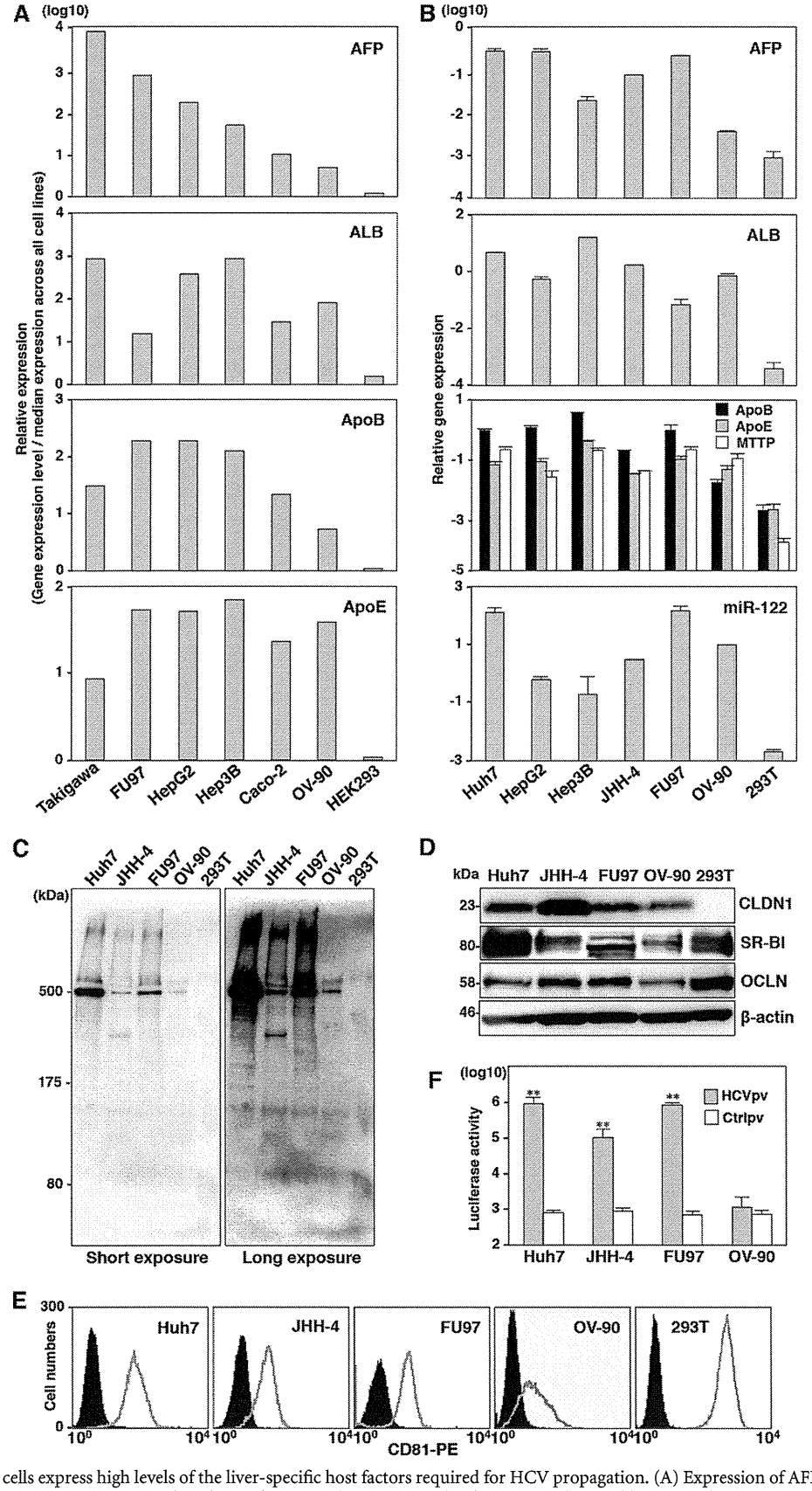

FIG 1 JHH-4 and FU97 cells express high levels of the liver-specific host factors required for HCV propagation. (A) Expression of AFP, ALB, ApoB, and ApoE in cancer cell lines screened by the NextBio Body Atlas application. The expression levels were standardized by the median expression across all cell lines. (B) Expression of AFP, ALB, ApoB, ApoE, MTTP, and miR-122 in AFP-expressing cell lines including HepG2, Hep3B, FU97, and OV-90 cells identified by NextBio

with respect to HCV RNA replication, *in vitro*-transcribed subgenomic HCV RNA of the Con1 strain was electroporated into Huh7 and FU97 cells and cultured in medium containing G418 for a month, and then subgenomic replicon (SGR) cells of the Con1 strain were established (Fig. 4A). Replication of HCV RNA in four clones of the FU97 replicon cells was examined by qRT-PCR and immunoblotting. All clones contained a high level of HCV RNA (3×10^7 to 7×10^7 copies/μg total RNA) (Fig. 4B, upper panel), and the NS5A protein was also detected (Fig. 4B, lower panel). We examined the localization of NS5A and dsRNA in clone 5 of FU97 SGR cells by immunofluorescence analysis. Colocalization of NS5A with dsRNA was observed in clone 5, suggesting that the replication complex required for viral RNA replication was generated in the FU97 SGR cells (Fig. 4C). It has been shown that the infectivity of HCVcc in the cured cells that were established by elimination of the viral genome by treatment with antivirals from Huh7 replicon cells is significantly higher than that in parental Huh7 cells (49). To establish FU97 cured cells, two clones of FU97 replicon cells (clones 5 and 7) were treated with a combination of either 100 IU/ml of IFN-α and 100 nM BILN 2061 (clones 5-1 and 7-1) or 10 pM BMS-790052 and 100 nM BILN 2061 (clones 5-2 and 7-2) to eliminate viral RNA. Viral RNA was gradually decreased and was completely eliminated at 26 days posttreatment in four clones (Fig. 4D), and elimination of NS5A expression in cured cells was confirmed by immunoblot analysis (Fig. 4E). Next, to examine the susceptibility of the cured cells to the propagation of HCVcc, FU97 cured cell clones (clones 5-1 and 7-1) and parental FU97 cells were infected with HCVcc at an MOI of 1. The cured cells are more permissive to HCV infection, resulting in increased HCV RNA (Fig. 4F) and NS5A abundances (Fig. 4G) compared to the parental cells. These results suggest that susceptibility of the cured FU97 cells to the propagation of HCVcc is higher than that of parental cells, as seen in previous studies using hepatic and nonhepatic cells (17, 18, 49).

Cured FU97 cells exhibit normal innate immune response. It has been shown that one of the reasons for the high susceptibility of the cured cell line, Huh7.5 cells, to HCVcc infection is the impairment of the innate immune responses caused by mutation in RIG-I, a key sensor for viral RNA (50). To examine the involvement of the innate immune response in the enhancement of HCVcc propagation in the cured FU97 cells, the expression levels of IFN-stimulated gene 15 (ISG15) were determined upon stimulation with IFN-α or infection with VSV. Expression of ISG15 was significantly increased in both parental and cured FU97 cells by treatment with IFN-α or infection with VSV (Fig. 5A). To further confirm the innate immune responses in the cured FU97 cells, reporter plasmids encoding the luciferase gene under the control of either the IFN-β (Fig. 5B, left) or ISRE (Fig. 5B, right) promoter were transfected into both parental and cured FU97 cells and treated with IFN-α or inoculated with VSV. Activation of these promoters in the cured cells was comparable to that in the parental cells. To further assess the authenticity of viral RNA recognition and ISG induction pathways in the cured cells, nuclear localization of IRF3 and STAT2 upon stimulation was determined by immunofluorescence analysis. IRF3 and STAT2 in both parental and cured FU97 cells were translocated at similar levels into the nucleus upon infection with VSV or treatment with IFN-α (Fig. 5C). These results suggest that the efficient propagation of HCVcc in the FU97 cured cells is attributable to reasons other than impairment of innate immunity.

Expression of miR-122 is one of the determinants for HCV RNA abundances. We hypothesized that HCV replicon cells are capable of surviving in the presence of G418 by amplification of the viral genome through the enhancement of miR-122 expression, and cured FU97 cells acquired the ability to propagate HCVcc due to the high-level expression of miR-122. Our previous study also suggested that the expression levels of miR-122 in Huh7, Hep3B, and Hec1B cured cells were higher than those in parental cells (17, 18). To test this hypothesis, the expression levels of miR-122 in the cured FU97 cells were compared with those in parental cells. Interestingly, the cured FU97 cell clones exhibited a 1.8-fold increase in miR-122 expression (Fig. 6A). These results suggested that the efficient propagation of HCVcc in the cured FU97 cells was attributable to enhanced expression of miR-122 rather than the impairment of the innate immunity. To further confirm the correlation between the expression of miR-122 and HCV RNA abundances, we established FU97 cell lines expressing various concentrations of miR-122 by using a lentiviral vector (Fig. 6B), and HCV RNA abundances in these cell lines upon infection with HCVcc were determined by qRT-PCR (Fig. 6C). HCV RNA abundances increased in accord with the expression of miR-122, suggesting that expression of miR-122 is one of the determinants for HCV RNA abundances in cells infected with HCVcc.

HCV particles produced in FU97 cells exhibit similar characteristics to those in hepatic cells. To examine the characteristics of viral particles produced in FU97 cells, HCV particles recovered from the culture supernatants of Huh7.5.1 and FU97 cells infected with HCVcc were fractionated by buoyant density gradient analysis. Previous reports indicated that viral RNA and infectious particles were broadly distributed, with peaks in fractions from 1.13 to 1.14 g/ml and from 1.09 to 1.10 g/ml, respectively (51, 52). In agreement with the previous data, major peaks of HCV RNA and infectious particles in culture supernatants of both Huh7.5.1 and FU97 cells were detected around 1.10 g/ml and 1.09 g/ml, respectively (Fig. 7A and 7B, upper panels). Furthermore, ApoE was detected around the peak fractions of infectivity in both Huh7.5.1 and FU97 cells (Fig. 7A and B, lower panels). These results suggest that HCV particles produced in FU97 cells exhibit characteristics similar to those in hepatic cells.

Effects of anti-HCV drugs on the propagation of HCV in FU97 cells. To determine the difference in the efficacies of antivirals on the HCV propagated in Huh7 and FU97 cells, three DAAs, i.e., BMS-790052, PSI-7977, and BILN 2061 targeting NS5A,

Body Atlas and Huh7, JHH-4, and 293T cells was determined by qPCR. The relative expression of AFP, ApoB, ApoE, MTTP, and ALB mRNA was normalized to that of glyceraldehyde-3-phosphate dehydrogenase (GAPDH) mRNA, and that of miR-122 was normalized to that of U6 snRNA. (C) Secretion of ApoB in the culture supernatants of Huh7, JHH-4, FU97, OV-90, and 293T cells was determined by immunoblotting by using anti-ApoB antibody. The molecular mass of ApoB100 secreted from hepatocyte is about 500 kDa. (D) Expression of CLDN1, SR-BI, and OCLN in these cell lines was determined by immunoblotting. (E) Expression of hCD81 in the cell lines was determined by flow cytometry. (F) HCVpv-bearing HCV envelope proteins and control virus (Ctrlpv) were inoculated into the cell lines, and luciferase activities were determined at 24 h postinfection. Asterisks indicate significant differences (*, $P < 0.05$; **, $P < 0.01$) versus the results for control virus.